Chem Soc Rev

REVIEW ARTICLE

View Article Online
View Journal | View Issue

Cite this: *Chem. Soc. Rev.*, 2015, **44**, 5320

Electrochemistry, biosensors and microfluidics: a convergence of fields

Darius G. Rackus,†[ab] Mohtashim H. Shamsi†[ab] and Aaron R. Wheeler*[abc]

Received 1st November 2014

DOI: 10.1039/c4cs00369a

www.rsc.org/csr

Electrochemistry, biosensors and microfluidics are popular research topics that have attracted widespread attention from chemists, biologists, physicists, and engineers. Here, we introduce the basic concepts and recent histories of electrochemistry, biosensors, and microfluidics, and describe how they are combining to form new application-areas, including so-called "point-of-care" systems in which measurements traditionally performed in a laboratory are moved into the field. We propose that this review can serve both as a useful starting-point for researchers who are new to these topics, as well as being a compendium of the current state-of-the art for experts in these evolving areas.

Introduction

We live in an era in which the traditional disciplines of chemistry, biology, physics, and engineering are intersecting and combining to form a dizzying array of new sub-fields and application-areas. For example, electrochemistry, biosensors, and microfluidics have become increasingly linked together, making it difficult to conceive of them as separate entities. As shown in the Venn diagram in Fig. 1, these intersections can be sub-divided into four application areas: (A) electrochemistry and microfluidics, (B) electrochemical biosensors, (C) microfluidic biosensors, and (D) microfluidic electrochemical biosensors. Here, we focus on the rich interplay between electrochemistry, biosensors, and microfluidics, with an emphasis on how they are combining to form new application-areas, including so-called "point-of-care" diagnostics, in which measurements traditionally performed in a laboratory are moved into the field.

The scientific literature is replete with in-depth discussions of electrochemistry,[1,2] biosensors,[3–5] and microfluidics.[6–8] This review is unique in that we focus on how these sub-fields overlap and work together, in two sections. First, we include three tutorials, defining the key terms and explaining the basic principles for electrochemistry, biosensors, and microfluidics.

[a] *Department of Chemistry, University of Toronto, 80 St. George St., Toronto, ON M5S 3H6, Canada. E-mail: aaron.wheeler@utoronto.ca*
[b] *Donnelly Centre for Cellular and Biomolecular Research, University of Toronto, 160 College St., Toronto, ON M5S 3E1, Canada*
[c] *Institute of Biomaterials & Biomedical Engineering, Rosebrugh Building, 164 College St., Toronto, ON M5S 3G9, Canada*
† Equal contributors.

Darius G. Rackus

Darius Rackus obtained his MSc in Chemistry and Biological Science in 2012 from the University of Durham and is currently pursuing a PhD in Analytical Chemistry at the University of Toronto under the supervision of Professor Aaron Wheeler. Current research activities involve integrating novel electrochemical sensors with digital microfluidics. Research interests include biosensors, clinical chemistry, and miniaturizing assays.

Mohtashim H. Shamsi

Mohtashim Shamsi obtained his doctoral degree under the supervision of Dr Bernie Kraatz and earned his PhD in the area of electrochemical DNA biosensors from the University of Toronto in 2012. He joined the Wheeler group as a postdoctoral fellow in 2012, where his research focus has been integration of electrochemical sensors in digital microfluidic chips. In fall 2015, he will join the faculty in the Department of Chemistry and Biochemistry at Southern Illinois University, Carbondale (SIUC). His research focus will encompass the interfaces between electrochemistry, biosensing and microfluidics.

Second, we review the current state-of-the-art in the overlapping areas (A, B, C, D), as outlined in Fig. 1. We propose that the fourth of these areas, microfluidic electrochemical biosensors (D), is a particularly attractive subject, with great promise for point-of-care diagnostics and other advances that are shaping the world that we live in.

Electrochemistry

Electrochemistry[1,2] is one of the oldest branches of chemistry, and has historically been used for studying heterogeneous electron transfer kinetics[11] (most commonly at a metal/solution interface), with applications in metallurgy,[12] corrosion science,[13] semiconductors,[14] fuel cells,[15] self-assembled coatings,[16] and electrochemical sensors.[7] The latter application, electrochemical sensing, has attracted wide attention because of two important advantages: inexpensive instrumentation and miniaturization. These advantages are typified by the use of systems relying on inexpensive potentiostats (*i.e.*, a control circuit used to apply electric potentials and measure small currents) and electrochemical cells formed by screen printing (*i.e.*, a scalable manufacturing technique capable of forming electrodes at low cost). These advantages constitute the driving forces behind the development of (now ubiquitous) point-of-care glucose monitors and alcohol sensors.[17]

We review here some of the fundamental terms and basic principles of electrochemistry. Electrochemical phenomena are often measured using a cell comprising three electrodes: (1) a working electrode (WE) where the redox reactions of interest occur and are measured, (2) a counter electrode (CE) that is controlled by the potentiostat to set the WE potential and balance current, and (3) a reference electrode (RE) that provides feedback of the WE potential to the potentiostat. The WE and CE are in direct contact with the solution being studied and the RE is often in indirect electrical contact by means of a conductive salt bridge. For analytical purposes, electrons should transfer across the solution/solid interface smoothly and rapidly; thus, great attention is paid to electrode size, geometry, material, and surface structure. While electrodes used in electrochemical measurements have traditionally had dimensions on the order of millimetres, micrometre-scale "microelectrodes" and "ultramicroelectrodes" have recently become popular in applications related to microfluidics and biosensing. Electrodes with these dimensions offer advantages such as the ability to measure small currents in the range of picoamperes to nanoamperes (pA–nA), rapid response to changes in applied potential, low ohmic reduction in electric potential, efficient diffusional mass transport, and steady-state response at diffusion-controlled potential. These advantages allow the efficient electrochemical study of organic systems, sensitive detection of ultralow concentrations of analytes, and measurements of ~μL sample volumes.

When an electrode with excess charge on its surface comes in contact with ions in solution, an electrical double-layer of ions (~5–20 nm thick) is formed at the surface. The layer closest to the electrode is called the inner layer, for which the excess charge on the electrode surface is balanced by an equal number of oppositely charged ions in solution. The second layer, known as the diffuse layer, is a group of oppositely charged ions with concentration that decreases exponentially as a function of distance from the inner layer. An electric potential exists between the two layers, defined by the amount of charge and the distance between them. In an electrochemical process, the species under investigation moves from bulk solution to the electrical double layer by one (or more) of three modes of mass transfer: (1) diffusion, the movement under the influence of a concentration gradient between the bulk solution and the electrode surface region, (2) migration, the movement under the influence of the potential gradient between the electrode surface and the bulk solution, and (3) convection, the forced movement by means of mechanical force (*e.g.*, stirring).

For most electrochemical applications, the analyte participates in a reduction–oxidation (or redox) reaction as consequence of an electric potential, E, that is measured between the WE and RE. The electric potential and the concentrations of species being oxidized or reduced (C_O, C_R) vary according to the Nernst equation (eqn (1)):

$$E = E^0 + \frac{RT}{nF}\ln\frac{C_O}{C_R} \quad (1)$$

where E^0 is the "standard" potential for the reaction, R is the universal gas constant, T is temperature, n is number of electron transfers involved in the reaction and F is Faraday's constant. In the most straightforward form of electrochemical sensing, potentiometry, the Nernst equation is used to discern C_O and/or C_R in a passive system (*i.e.*, one with no external potential applied). A powerful application of potentiometry is the use of an ion-selective electrode for highly selective measurement of E for one species by means of a synthetic ion-specific coating. There are many other electrochemical techniques, but three of them, amperometry, voltammetry and electrochemical impedance spectroscopy, are most commonly used with microfluidics and/or for biosensing applications.

Aaron R. Wheeler

Aaron Wheeler earned his PhD in Chemistry at Stanford University in 2003. After a postdoctoral fellowship at UCLA, he joined the faculty at the University of Toronto in 2005, where he is the Canada Research Chair in Bioanalytical Chemistry. Wheeler's research group develops microfluidic tools to solve problems in chemistry, biology, and medicine. Wheeler has been recognized with a number of honors including the W.A.E. Mcbryde Medal from the Canadian Society for Chemistry, the Arthur F. Findeis Award from the American Chemical Society, and the Joseph Black Award from the Royal Society of Chemistry.

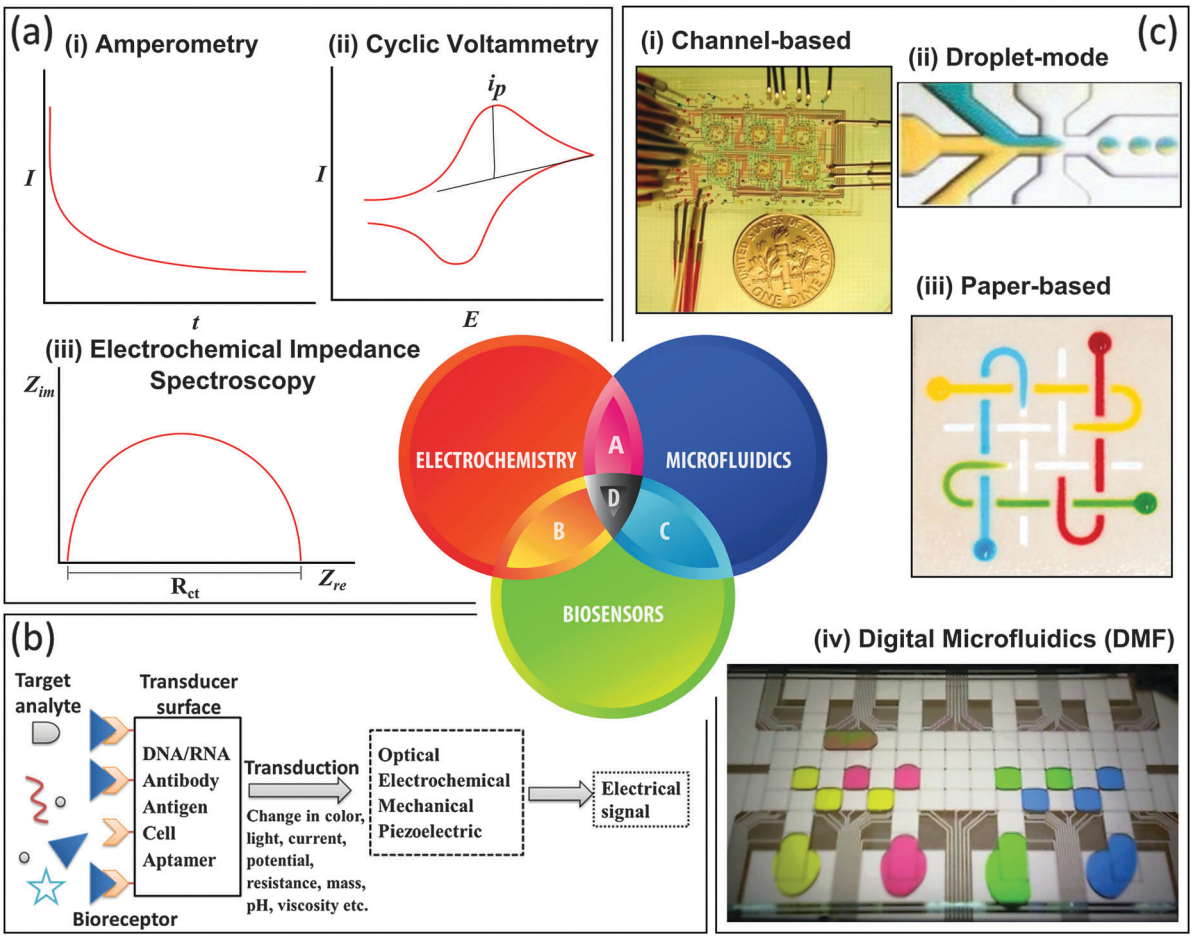

Fig. 1 Electrochemistry, biosensors, and microfluidics. (a) Electrochemistry – (i) representative amperometry response plot, (ii) representative cyclic voltammogram, and (iii) representative electrochemical impedance spectroscopy Nyquist plot. (b) Biosensors – schematic of a representative biosensor, coupling biomolecular recognition to signal transduction. (c) Microfluidics – (i) picture of a microchannel-based device reprinted from Balagaddé *et al.*[9] [*Science*, 2005, **309**, 137–140], reprinted with permission from AAAS, (ii) picture of a droplet microfluidic device reprinted with permission from Dolomite Microfluidics, Charlestown, MA, USA, (iii) picture of a paper microfluidic device adapted from Martinez *et al.*,[10] copyright (2008) National Academy of Sciences, USA, (iv) frame from a video depicting actuation of coloured droplets on a DMF platform.

Amperometry is an electrochemical analysis mode in which current is measured while a constant external electric potential is applied between the WE and CE. The current I is recorded as a function of time t, as shown (for a system with no convection or migration) in Fig. 1(a)i. Because electron transfer can only occur in very close proximity to the electrode, the current at the WE is proportional to the flux of analyte to the electrode surface which depends linearly upon the concentration gradient of the analyte between the surface and the bulk solution. Initially, only the analyte near the double-layer is depleted (*i.e.*, oxidized or reduced), resulting in high current. As the current continues to flow, the region of reduced analyte concentration extends further into the solution; thus, the concentration gradient declines with time, which causes the current to decline. Since the progression of the concentration gradient depends on the concentration of analyte in the bulk solution, the time dependence of the magnitude of the current that is measured can be related to the concentration of analyte in solution.

Voltammetry is the most extensively used technique in electrochemistry, partly because it can probe the reversibility of the system under study. Like amperometry, in voltammetry, an electric potential E is applied between the WE and CE and the resulting current I is measured. Unlike amperometry, in voltammetry, E is varied as a function of time. For example, in the (most common) format of cyclic voltammetry, E is swept in a linear cycle at scan rate v. As shown in Fig. 1(a)ii, as E becomes more positive, the analyte becomes oxidized, and as E becomes more negative, the analyte becomes reduced, with each step (oxidation and reduction) associated with a peak current, i_p. The relationship between i_p and v is given by the Randles–Sevcik equation (eqn (2)):

$$i_p = (2.69 \times 10^5) ACD^{1/2} n^{3/2} v^{1/2} \quad (2)$$

where A is the electrode area, C is the concentration of analyte in bulk solution, D is the diffusion coefficient of the analyte, and n is the number of electrons involved in the reaction. The magnitude of i_p can be used to determine analyte concentration, and the

potentials at which the analyte is oxidized/reduced can be used for qualitative identification. Peak currents can be enhanced by means of redox cycling whereby the species of interest that is being oxidized or reduced at the electrode surface is regenerated (and thus measured repeatedly) either chemically, enzymatically, or electrochemically.

Voltammetric methods also include linear sweep voltammetry, differential pulse voltammetry, square-wave voltammetry, AC voltammetry, and stripping voltammetry. Stripping voltammetry, in particular, is used widely in sensing applications for trace detection. Analytes are electrochemically immobilized (deposited or adsorbed) on the electrode surface by reduction, oxidation, or other adsorption processes, allowing for accumulation of low-concentration species as a function of time. Subsequent sweeping of the potential then strips off the analyte, resulting in a peak current that correlates with the original analyte concentration.

Electrochemical impedance spectroscopy (EIS) is a powerful electrochemical method that has recently become popular in biosensing because of its capability to detect binding events on a transducer surface. In EIS, a DC potential E_{DC} and a small sinusoidal AC perturbation (E_{AC}, $\sim$5–10 mV amplitude) are applied between the WE and the RE. The magnitude and the phase angle ϕ of the resulting current I are recorded as a function of the AC frequency. The current magnitude can be converted into impedance Z using Ohm's law ($Z = V/I$), and impedance is expressed as a complex number $Z = Z_{re} + jZ_{im}$ where real impedance Z_{re} has $\phi = 0$ (*i.e.*, is independent of frequency) and imaginary impedance Z_{im} has $\phi \neq 0$ (*i.e.*, is dependent on frequency). The data generated by EIS is often presented as a Nyquist plot of Z_{im} relative to Z_{re} at different frequencies. As shown in Fig. 1(a)iii, at very high frequencies (left side of the plot) and very low frequencies (right side of the plot) there is no contribution from Z_{im}; at the low-frequency limit, $Z_{re} = R_{ct}$, the charge-transfer resistance. R_{ct} represents the diffusion-controlled limit for the redox reaction rate at the electrode surface (in biosensing, this property can be related to analyte concentration), and the maximum of the "semicircular" response at moderate frequencies is related to the capacitance of the double-layer. EIS is thus often used in characterizing the properties and behaviour of modified electrode surfaces and to extract the capacitive and resistive components of such surfaces using equivalent circuit models.[18]

Biosensors

The concept of a "biosensor" has been defined in many different ways in the literature.[3–5] Nearly all parties can agree that the definition should include (a) a biomolecular recognition element to confer selectivity, and (b) a signal transduction element to enable quantitative or semi-quantitative analysis. There are some who also insist that the biorecognition element should be positioned physically adjacent to the transducer.[19] We appreciate the reasons for this definition and agree that it is useful in some circumstances, but here we employ a broad definition of biosensor that incorporates any method coupling (a) to (b), regardless of the physical location of the individual components.

An ideal biosensor is selective, rapid, reusable (or reversible), portable, and requires minimal sample processing prior to analysis. There are few biosensors that achieve this in practice – trade-offs are almost always required. Fig. 1(b) depicts a generic biosensor scheme. As shown, the interaction between analyte molecules and the biorecognition element (in this example, a layer of bioreceptor molecules) causes transduction of a measurable physicochemical change such as current flow, heat transfer, or change in mass or refractive index.

Biorecognition elements in biosensing can be broadly classified in terms of the nature of their interaction with analyte molecules. An affinity biosensor operates as a function of permanent or semi-permanent binding between the biorecognition element and the analyte. This class of biosensors includes immunosensors (antibody–antigen binding), nucleic acid biosensors (probe and complementary nucleic acid target binding), and aptamer biosensors (ligand and synthetic oligonucleotide receptor binding). In contrast, in catalytic biosensors, the interaction between the analyte and the biorecognition element is impermanent, and involves a chemical reaction that forms an easily detected product. This class of biosensors includes enzymatic biosensors, cell-based biosensors, and biosensors relying on catalytically active polynucleotides (DNAzymes).[20] Catalytic systems are particularly useful for trace analysis because of the inherent amplification; *i.e.*, the presence of a single analyte molecule can result in a large number of products to be detected.

Signal transduction techniques in biosensing can be broadly classified in terms of whether the process requires labels, or whether the process is label-free. Biosensors that require labels are designed to transduce the analytical signal from a designated reporter molecule (not the analyte molecule itself). The label-format allows for flexible implementation of biosensing in a wide range of detection schemes, but a trade-off is the time, cost, and additional steps associated with incorporating reporter molecules into the process. In label-free biosensors, the signal is transduced directly from the presence of the analyte molecule itself. Some electroanalysis techniques (described above) as well as surface plasmon resonance and mass-sensitive techniques (described below) fall into this category. Label-free biosensors require very specific formats, but are advantageous in that reporter molecules are not required.

Biosensors (particularly when viewed in context of the definition used here) are remarkably diverse, comprising a wide range of combinations of biorecognition and transduction. Here we review common examples of each of these fundamental aspects of biosensing.

Biorecognition. Enzyme-based biosensors are catalytic sensors in which the bioreceptors comprise enzyme molecules in solution or tethered to a surface. Enzyme-based biosensors are typically implemented in direct or indirect format. In the direct format, the analyte promotes the activity of an enzyme (either acting as a co-factor for the enzyme or in concert with an affinity binding event to localize the enzyme near the analyte), which catalyzes the formation of a measurable product (*i.e.*, analyte concentration is

proportional to signal). In the indirect format, the analyte inhibits the activity of the enzyme, resulting in reduced rates of formation of a measurable product[21] (*i.e.*, analyte concentration is inversely proportional to signal).

Immunosensors are affinity-based biosensors that rely on the binding of an antibody to its specific antigen. Immunosensors are implemented in a variety of schemes, including (a) direct format, featuring binding of an unlabeled antigen to an unlabeled antibody (requiring label-free transduction), (b) competitive format, featuring competition for binding of an unlabeled (target) antigen and a labeled (exogenous) antigen to an antibody, (c) ''sandwich'' format featuring an antigen with two epitopes (*i.e.*, antibody-recognition sites) that binds to an immobilized primary antibody and also to a labeled- or enzyme-modified secondary antibody (when the secondary antibody is enzyme-modified, the technique is known as an ''enzyme-linked immunosorbent assay,'' ELISA – this is likely the most common immunosensor format), and (d) inhibition format featuring competition between an analyte and a primary antibody for binding to a labeled (or enzyme-modified) secondary antibody. Immunosensors are likely the most common form of biosensors, primarily a function of the flexibility of the biorecognition; antibodies can be raised to selectively bind proteins (including enzymes and other antibodies), small molecules (including hormones, toxins, environmental contaminants), cells (including surface-markers on pathogenic bacteria), and many other classes of antigen.

Nucleic acid-based biosensors are affinity sensors that exploit the sequence-specific Watson–Crick base pairing between nucleic acids and their complements. The most common form of nucleic acid sensors are formed from a single-stranded DNA (ss-DNA) probe that is immobilized onto the surface of a transducer. Upon recognition of its complementary ss-DNA or RNA analyte (or target) by hybridization, transduction is facilitated by optical, electrochemical, or mass-sensitive techniques. A well-known example of a (highly multiplexed) nucleic acid-based biosensor is the DNA microarray, which enables semi-quantitative analysis of gene expression for thousands of sequences in one shot.[22] There are a number of variations on the simple DNA-probe–DNA-target theme. One variation uses peptide nucleic acid (PNA) probes, in which the negatively charged sugar-phosphate backbone of DNA is replaced by a neutral pseudopeptide chain. PNA probes have higher binding affinities (relative to their analogous ss-DNA probes) for ss-DNA targets, and the reduced charges on these probes confer advantages for some forms of electroanalysis. Another variation is the sandwich assay, in which an immobilized probe binds a region of an analyte, and a second, labeled probe binds a different region of the analyte. A third variation known as a ''molecular beacon'' features probe-sequences that self-bind to form stem-and-loop or hairpin structures. Complementary targets compete for binding with such structures (requiring the probe to undergo a change in conformation) which can enable very sensitive detection of small numbers of targets. The most useful nucleic acid biosensors allow for differentiation between the binding of a target that is perfectly complementary to the probe and a target that has a one base-pair mismatch with the probe. This level of selectivity is required to identify single nucleotide polymorphisms (SNPs); there is great interest in using SNP detection to identify patients with genetic diseases.

Aptamer-based biosensors feature an alternative form of affinity biorecognition relying on synthetic oligonucleotide (single-stranded DNA or RNA molecules) probes; in contrast to conventional nucleic acid sensors (which bind only their complements), aptamers can be designed to bind any type of target. Aptamers are prepared by a combinatorial approach called systematic evolution of ligands by exponential enrichment (SELEX).[23] SELEX is an iterative process in which (1) a pool of oligonucleotides with varying sequences is generated, and (2) the population that binds best to a given target is selected and isolated. The best binding sequence(s) then serve(s) as the basis to generate new sequences, and steps (1)–(2) are iterated for several rounds to generate a product with high specific binding to the desired target. Aptamers modified with electroactive indicators, fluorescent tags, nanoparticles and enzymes have been used for amplified detection[24,25] of a wide range of targets including amino acids, antibiotics, co-factors, drugs, metal ions, nucleic acids, and organic dyes.

Transduction. Electrochemical transducers used in biosensing exploit the redox activity of a solute in solution – either the analyte itself, an electroactive label attached to the analyte, or a catalytically generated electroactive reporter. The electrons generated in the redox process are detected as current, which is related to the number of redox species involved in the process. In some instances, an electron transfer mediator is used to shuttle electrons from the electroactive species to the electrode surface (*e.g.*, from the redox centre of an enzyme to the electrode). Electrochemical measurement systems, which are ubiquitous in modern society in the form of portable glucose monitors, represent the most common form of transduction used in biosensing. As described in the preceding section, the most common electrochemical biosensors transduce signals by means of amperometry, voltammetry, or EIS. Amperometric and voltammetric sensors are often used in catalytic mode; for example, in amperometric glucose sensors, the WE is coated with a layer of glucose oxidase. When glucose in a blood sample encounters the enzyme, hydrogen peroxide is formed, which is then oxidized at the WE to generate a current that is proportional to the amount of glucose in blood. EIS, on the other hand, is often used for affinity biosensing, in which bioreceptors such as antibodies or nucleic acids are attached to the WE surface. In this scheme, the charge transfer resistance experienced by an electroactive reporter as it diffuses through the film of bioreceptors is a measure of the amount of bound analyte and the charge on the surface.[26] A disadvantage of EIS is its high sensitivity towards nonspecific adsorption.

Optical techniques represent another very common form of signal transduction used in biosensing.[20] While many analytes are optically active, optical transduction in biosensing often requires a label – one that binds to the analyte or one that is generated catalytically. The simplest optical sensing technique is absorbance (also known as colourimetry when used with

visible wavelengths), in which the relative intensity of light before and after passing through a sample correlates with the concentration of absorbing species (also known as chromophores) in the sample. In the related (and more sensitive) technique of fluorescence (or fluorimetry), the light that is detected is emitted from fluorescent species (also known as fluorophores) after the initial absorption (or excitation). The wavelengths of light that are absorbed and emitted match differences between electronic energy levels of the chromophores and fluorophores. In some cases, a fluorophore may be ''quenched'' by the presence of other species that allow the excited fluorophores to relax non-radiatively. Some biosensors are designed to take advantage of this effect, such that when analytes bind, a fluorophore and quencher become more or less associated (which changes the amount of emitted light). A related effect known as Förster resonance energy transfer (FRET), involves two fluorophores, a ''donor'' and an ''acceptor.'' The relative intensities of emitted light generated from the two fluorophores varies as a function of the distance between them, making FRET a useful tool for probing recognition events that result in a change in probe conformation (as in molecular beacons, described above). A disadvantage of absorbance and fluorescence transduction is the requirement of an external light source; an alternative known as chemiluminescence, often used in catalytic biosensors to generate chemiluminescent reporter molecules, does not require an external light source. All optical analysis techniques require an optical transducer such as a photodiode or photomultiplier tube (PMT), and they often require lenses, reflectors, and other optical components.

Surface plasmon resonance (SPR) is a transducer that is often used in label-free affinity biosensing. In SPR, light from an external source is reflected off of a metal film, generating an evanescent wave that penetrates a short distance into the film. When the energy of the light matches that of the surface plasmons (*i.e.*, coherent oscillations of electrons at the metal-external medium interface), the energy from the incident light is transferred into the surface plasmons.[27] This effect is typically evaluated by monitoring the wavelength or angle at which the energy is transferred, observed as a ''dip'' in the intensity of the reflected beam. The surface plasmon resonance energy depends on the refractive index of the medium adjacent to the metal film; thus, if the surface is modified with receptor molecules and the receptors bind analyte molecules, the shift in resonance angle or wavelength provides a real-time signal that corresponds with analyte concentration.[28] Nanostructuring the thin metal surface improves signal by exciting the various modes of SPR and long-range surface plasmons.[29] Surfaces can be imaged by SPR using a technique known as SPR imaging (SPRi). SPRi is performed by holding both the wavelength and the angle constant and measuring the reflectance across a sample surface.[30]

Mass-sensitive detectors represent a final class of transducers that are commonly used in biosensing. The most common forms of these sensors rely on piezoelectric substrates – that is, materials (including some ceramics and quartz crystals) that can convert electrical into mechanical energy and *vice versa*. The two most common mass-sensitive analysis techniques are surface acoustic wave (SAW) sensors and quartz crystal microbalance (QCM) sensors. In the former (SAW), an AC excitation signal is applied to the surface of a piezoelectric substrate to generate a SAW with characteristic velocity v. After propagating across a sensing area, the properties of the wave are interrogated and compared to the excitation signal. The velocity of the wave depends on the density of molecules on the surface of the substrate; thus, the technique can be used to probe the mass of analyte molecules bound to bioreceptors on the surface.[31] QCM is similarly mass-sensitive, evaluating the shift in resonant frequency Δf for a standing wave applied through the bulk of a piezoelectric substrate, which (like SAW) depends on the mass of analyte molecules bound to the surface.[32] The resonant frequency is inversely proportional to the crystal thickness and the addition of mass on the surface can be treated as an extension of the crystal thickness. A third mass sensitive transducer is the microcantilever, which derives its origins from atomic force microscopy. Binding of the analyte to a biological recognition layer on the microcantilever induces surface stress resulting in nanomechanical motion. This motion can be monitored optically or by a piezoresistive readout system.[33] A limitation of mass-sensitive detectors is an inherent sensitivity to non-specific adsorption onto the surface.

Microfluidics

Microfluidics is a technology that facilitates the manipulation of small volumes of fluids in the range of μL–aL (10^{-6} to 10^{-18} liters).[6–8,34] Microfluidics is most often implemented in planar substrates bearing enclosed channels with lengths, widths, and depths on the ~10 mm, ~100 μm, and ~10 μm scales, respectively. The technology was popularized in the early 1990s[35,36] for applications related to chemical separations, but in the intervening years it has been applied to an incredible array of applications, ranging from genomics[37] and synthesis[38,39] to music[40] and mazes.[41,42] A particularly attractive vision for the microfluidics community has been the development of integrated ''lab on a chip'' systems that reproduce laboratory-scale processes with reduced cost, less time, and with substantially smaller footprints than their conventional counterparts.[43] A highly regarded journal with the same name was founded in 2000, and now publishes >600 papers in 24 issues per year.

The micrometer dimensions that are common in microfluidics result in fluidic phenomena that exhibit increased importance of viscosity, surface tension, and diffusion when compared to conventional systems. These properties are often represented in terms of dimensionless parameters, including Reynold's number (Re, eqn (3)), Capillary number (Ca, eqn (4)), and Péclet number (Pe, eqn (5))

$$\mathrm{Re} = \frac{\rho l v}{\mu} \tag{3}$$

$$\mathrm{Ca} = \frac{\mu v}{\gamma} \tag{4}$$

$$\mathrm{Pe} = \frac{v l}{D} \tag{5}$$

where ρ is fluid density, l is a characteristic length in the system, v is mean fluid velocity, μ is dynamic fluid viscosity, γ is surface tension, and D is coefficient of diffusion. In general terms, Re, Ca, and Pe are low for microfluidic systems, meaning that viscous forces dominate inertial forces (resulting in laminar flow), interfacial forces dominate viscous forces, and diffusion dominates convection. These phenomena are important to consider when designing microfluidic systems for biosensors and electrochemistry. For more, there are a number of reviews[44,45] and textbooks[46,47] that describe fluid phenomena at micron length dimensions in great detail.

Microfluidic platforms can be classified into a number of different categories, including (1) channel-based microfluidics, (2) paper-based microfluidics and (3) digital microfluidics. There are many alternative classifications (*e.g.*, one might include a SlipChip[48] category, or split a "droplet microfluidics" category out from "channel-based microfluidics"), but these categories suffice for the purposes of this review. We describe each of them below.

Channel-based microfluidics. In its original conception, the technology of "microfluidics" was coincident with "microchannels," and channel-based microfluidics continues to represent (by far) the most widely practiced category of microfluidics. Initial work with microchannels focused on the translation of the electrokinetic flow techniques (*e.g.*, electroosmosis and electrophoresis) used in capillary electrophoresis to networks of microchannels to effect chemical separations.[49] Electrokinetic flow is particularly advantageous because there is very little external equipment required (*i.e.*, only a high-voltage power supply), but the range of reagents and solvents that can be used is limited. Other forms of fluid manipulation soon followed, including various types of pressure-driven flow controlled by external pumps, centrifugal forces,[50] or on-chip peristaltic pumps.[51] These techniques are amenable for working with a wide range of reagents, but they each (to varying degrees) require ancillary equipment to operate. Microchannel device materials are an important concern – for example, polymer materials that can be molded such as polydimethyl(siloxane) (PDMS) are straightforward to fabricate, but have limited chemical compatibility, while hard materials like glass and silicon have greater chemical compatibility but typically require access to specialized instrumentation and are more time-consuming to fabricate.[52]

Microchannel-devices are operated in either continuous mode (often with integrated valves and pumps as in Fig. 1(c)i, or droplet-mode, as in Fig. 1(c)ii). The laminar flow-characteristics of the former (with its inherently low Re) has been exploited for a wide range of applications involving intricate chemical gradients.[53,54] The latter, which is implemented by combining immiscible solvents in microchannels to form emulsions (often aqueous droplets in an oil carrier-phase), has recently exploded in popularity, with seemingly endless examples of applications.[55–57] Microchannel droplet systems can be operated at extremely high-throughput (generating more than 10^3 droplets per second[58]), and are particularly well-suited for sorting applications.[59] There has been some progress developing methods that allow for individual droplet addressing and manipulation,[60,61] but the strength of the technique is in throughput rather than individual droplet control. The application for droplet microfluidics that has likely attracted the most attention is "digital PCR," in which a sample is dispensed into millions of droplets, allowing massively parallel amplification and measurement, which affords orders of magnitude greater precision and sensitivity relative to conventional PCR.[62]

Paper-based microfluidics. Paper-based microfluidics is an alternative scheme for miniaturized fluid handling in which liquid samples are passively wicked (or "pumped") by lateral flow through paper substrates. The Whitesides group popularized this phenomenon as being a member of the "microfluidics" family in 2007,[63] but similar ideas have been used for many decades[64] and indeed, products relying on lateral flow are widely available to consumers in the form of pregnancy tests. Paper microfluidic devices (in their modern format) are implemented by forming hydrophobic/hydrophilic patterns to guide fluid movement through paper (Fig. 1(c)iii). A variety of creative techniques have been developed to form such patterns including wax printing,[65] inkjet printing,[66] photolithography,[67] flexographic printing,[68] and many others;[69] paper can also be cut to a specific geometry to guide fluid movement.[70] Paper microfluidics has become popular because of the very low cost, ease of fabrication, flexibility, disposability, and the convenience of liquid transport without applying an external driving force. For these reasons, there is great enthusiasm for using paper microfluidics for point-of-care diagnostic assays,[71] with particular interest in their use as a low-cost platform for delivering medical diagnostics in resource-limited settings.[72]

The paper microfluidic concept has been implemented in formats ranging from simple dipstick assays in which a single reagent adsorbed on a paper substrate changes colour after contacting an analyte (*e.g.*, pH strips), to sophisticated microfluidic paper-based analytical devices (μPADs) relying on multilayer substrates including some or all of (a) a membrane modified with biorecognition agents, (b) a pad designed to absorb sample, (c) conjugate pads which are preloaded with conjugated particles – *e.g.*, gold nanoparticles, (AuNPs), *etc.*, (d) a wicking or an absorbent pad to provide capillary driving forces, and (e) a backing that provides mechanical stability.[73,74] Detection is typically implemented by electrochemistry or colourimetry (consistent with low-tech, portable applications), but paper microfluidic systems have also been reported that use chemiluminescence[75] and electrogenerated chemiluminescence.[76] Despite these advances, paper-based microfluidics lags the other categories of microfluidics in quantitative performance; there is room for improvement in selectivity, specificity, sensitivity, and linear dynamic range.[73,77]

Digital microfluidics. Digital microfluidics (DMF) is a third category of microfluidics, in which samples are manipulated as discrete droplets on a flat surface.[7,78–80] The most common implementation of digital microfluidics relies on electrostatic forces generated on arrays of electrodes coated with a hydrophobic insulating layer. In this format, droplets can be made to move, merge, mix, split, and be dispensed from reservoirs. These operations and others can be called iteratively (as in computer programming) to execute sophisticated, multi-step assays. While the other

forms of microfluidics are compatible with similar operations, DMF is unique in enabling them on devices with a generic format (Fig. 1(c)iv) that can be used and reused for very different applications. Moreover, the capability to address each individual droplet allows for complete control over reagent/sample state, position, and activity.

The most common digital microfluidic systems rely on electrostatic forces, which are often described in terms of "electrowetting," in which Laplace pressures are applied as consequence of asymmetric changes in droplet shape.[81] The electrowetting analogy is useful for modeling conductive liquids with high surface tensions, but droplet actuation can be described more generally using the Maxwell Stress Tensor[82] or electromechanical lumped-sum models.[83] Historically, DMF devices were rigid, formed from hard materials such as glass and silicon, but a recent trend is the formation of paper-based devices using inkjet printing.[84,85] One barrier to entry for users adopting DMF is the need for a custom, highly parallelized control system capable of handling high voltages. The recent development of an "open-source" control system[86] mitigates this to some extent. As an alternative to electrostatic control, alternative DMF systems can be realized using magnetic,[87] optical,[88] acoustic,[89] or thermocapillary[90] forces.

Digital microfluidics is complementary to the other forms of microfluidics. For example, DMF is advantageous in that there are no pumps, valves, interconnects, or fittings; on the other hand, the throughput of DMF is much lower than that of droplets-in-channels (note that DMF throughput may improve significantly with the development of devices formed from arrays of thin film transistors[91]). DMF is particularly well suited for applications involving solids (*e.g.*, tissue,[92] dried blood,[93] hydrogels,[94] monoliths[95]), as there are no microchannels that might become clogged. Indeed, methods that use magnetic forces to control large (solid) boluses of magnetic particles combined with electrostatic droplet control over droplet position is emerging as a powerful method for implementing immunoassays.[96–100]

A convergence of fields

Here we review a selection of representative applications in each of the overlapping areas defined in the Venn diagram in Fig. 1: (A) electrochemistry and microfluidics, (B) electrochemical biosensors, (C) microfluidic biosensors, and (D) microfluidic electrochemical biosensors.

A. Electrochemistry & microfluidics

Among all the analytical techniques coupled with microfluidics, electrochemical detection is the simplest to integrate, which makes it ideal for point-of-care applications (as reviewed by Sassa *et al.*[101]). In this section we discuss the incorporation of electrochemical detection with the various modalities of microfluidics.

Microchannels. The integration of electrochemical detection with microchannels dates back to the early days of microfluidics when microchannels were primarily used for electrophoretic separations. Originally, amperometric detection methods for separations were used for such applications,[102,103] which was followed by the incorporation of voltammetric methods to detect a variety of organic and inorganic analytes.[104]

Typically, microfluidic systems incorporating electrochemical detection are implemented by patterning electrodes on a flat glass or silicon substrate, and then a polymer-based substrate bearing microchannels is adhered to this substrate.[105] Glass and silicon are common substrates for electrode fabrication, but inexpensive alternatives such as compact discs can also be used.[106] In some cases, discrete REs and CEs are inserted into channel inlets. REs can also be incorporated within channels by means of a salt bridge,[107,108] as depicted in Fig. 2(a). The performance of electrodes within a microchannel depends on a variety of parameters including electrode position and flow rate.[109]

Examples of separations coupled with electrochemical detection include the isolation of hydrolysis products,[110] the monitoring of biomolecule release from individual cells,[111] and the quantitation of bioactive molecules in serum.[112] The main challenge in integrating electrochemical detection with electrophoretic separations has been isolating the separation and detection modules. Several strategies have been employed to overcome this problem, including the placement of the WE within the channel,[113] the use of a decoupler that shunts electrophoretic current away from the electrochemical cell,[114] floating the potentiostat ground,[115] wirelessly isolating the potentiostat,[116] or using an in-channel salt-bridge.[108]

Microchannel devices have also been found useful for cell culture affording reduced volumes and precise control over the extracellular environment. This makes them ideal for studying cell-to-cell signaling including neurotransmission. For example, microfluidics and electrochemistry have become popular in neuroscience because of the electroactive nature of (some) neurotransmitter analytes.[117,118]

Reusable electrodes can be incorporated with microfluidic systems using a modular approach. Using 3D printing, Erkal *et al.*[119] fabricated microchannel devices with threaded receiving ports where electrodes could be integrated. This allows the user to remove and polish the electrodes in between experiments when electrode surface-fouling is observed. This modular approach to integration was coupled with flow injection analysis of dopamine and monitoring ATP concentrations in cell culture studies.

Paper microfluidics. Coupling of electrochemistry with paper microfluidics is attractive as it combines two low-cost technologies for the prospect of inexpensive diagnostics and point-of-care testing. Two strategies for integrating electrochemical detection with paper microfluidics are (1) printing electrodes from conductive inks using screen printing (Fig. 2(b))[120,123] or inkjet printing,[124] and (2) coupling external electrodes to the paper microfluidic devices. The simplest approach for the latter is to affix a three-electrode assembly directly to a paper device.[125–127] Alternatively, microwire electrodes can be incorporated in both conventional microchannels and paper/lateral flow devices, which can be affixed using adhesive tape (Fig. 2(c)).[121]

Paper microfluidic devices integrated with electrochemical detection have been used for separations,[127,128] and quantitation

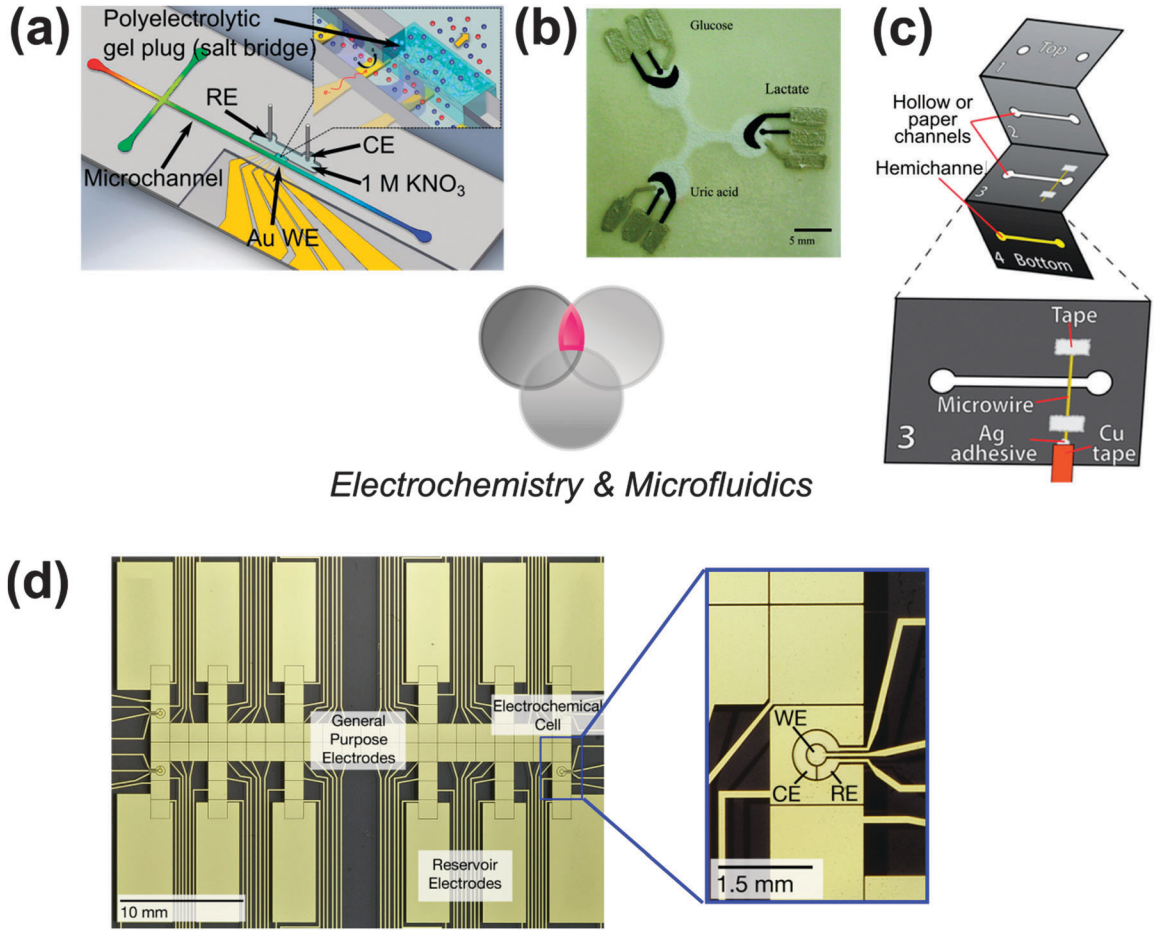

Fig. 2 Electrochemical detection in microfluidics. (a) Cartoon of a microfluidic channel with a polyelectrolytic gel salt bridge isolating the RE from the main channel. The Au WE is patterned onto the channel substrate. Wires in a 1 M KNO_3 solution are separated from the microchannel by a salt bridge. Reprinted with permission from Kang *et al.*,[108] copyright 2012 American Chemical Society. (b) Photograph of screen printed electrodes on a paper microfluidic device. The microfluidic device divides the sample into three aliquots which are then analyzed for glucose, lactate, and uric acid. Reprinted with permission from Dungchai *et al.*,[120] copyright 2009 American Chemical Society. (c) Cartoon of a folded paper microfluidic device with hollow channels. Electrodes are incorporated by taping microwires to the device. Ag adhesive and Cu tape are used for electrical contacts. Reprinted with permission from Fosdick *et al.*,[121] copyright 2014 American Chemical Society. (d) Photograph and schematic of electrodes incorporated into the bottom plate of a DMF device. Reactions and sample preparation take place in a general purpose area on the DMF device. A three-electrode electrochemical cell is patterned and insulating coatings are removed. Adapted with permission from Dryden *et al.*,[122] copyright 2013 American Chemical Society.

of metals[74,125,129] and bioactive molecules such as glucose, lactate, cholesterol, and uric acid.[120,130] In one unique example, Renault *et al.*[131] used screen printed electrodes formed in a multilayer paper device bearing microchannels. This device was shown to be versatile for a variety of voltammetric and amperometric analyses. Pressure driven flow, not typically used in paper microfluidics, was exploited to couple convection with electrochemical detection.

Digital microfluidics. In DMF, electrochemical detection can be implemented using external electrodes or by patterning the electrodes into the device, itself. The first report of electrochemistry coupled with DMF was a one-plate device used to detect the product of Greico's reaction in an ionic liquid droplet microreactor.[132] The device used two suspended gold wires as a ground electrode and the WE, respectively. However, this and other one-plate DMF/electrochemistry systems[133,134] suffer from the challenges of manual positioning of the electrochemical electrodes, liquid evaporation and the limited range of droplet operations compatible with one-plate DMF devices. These challenges can be overcome by using a two-plate DMF format where detection electrodes are either incorporated into the top or bottom plate of a DMF device.

Recently, two examples of integrating electrochemical analysis electrodes in the bottom plate of a two-plate DMF device were reported. Dryden *et al.*[122] integrated a three-electrode system within a gold layer used to form DMF actuation electrodes, as shown in Fig. 2(d). The photoresist SU-8 was used as the dielectric insulator on the bottom plate so that apertures could be opened over the electrochemical electrodes for sensing. The RE was electroplated with silver to provide a stable reference potential. This device was used for the quantification of acetaminophen by linear sweep voltammetry. In an alternative approach, Yu *et al.*[135] used reactive ion etching (RIE) to expose sensing electrodes on the bottom plate of a DMF device. The electrochemical cell comprised Au interdigitated WE and CE

and a small rectangular Au RE, all embedded within a driving electrode.

A second approach to integrating electrochemical detection in a two-plate DMF device is to pattern sensing electrodes on the top plate, which contains a thin conductive layer (often transparent ITO). This circumvents the need to pattern the dielectric insulator (a challenge for using electrodes embedded in the bottom plate, as above) and only the hydrophobic layer requires patterning. Shamsi *et al.*[97] used patterned ITO for the sensing electrodes. Most of the top plate was covered with a hydrophobic Teflon-AF layer, except the sensing electrodes which were exposed through a lift-off process. The exposed ITO was electroplated with Au to serve as the WE and Ag as a pseudo-RE. Alternatively, Yu *et al.*[136] used Au electrodes for grounding and sensing on the top plate of a DMF device. In this configuration, the ground electrode was patterned as a thin trace to maintain visibility. This format restricts droplet movement to patterns that match the ground electrode.

B. Electrochemical biosensing

Electrochemistry has been linked to biosensing since the concept of the latter was first proposed. In fact, the first biosensor, described by Clark and Lyons[137] in 1962, was an electrochemical oxygen sensor, with selectivity for glucose conferred by a layer of glucose oxidase. Electrochemical biosensors can be categorized either by the type of electrochemical technique or on the basis of the biorecognition element (*i.e.*, catalytic or affinity). There are good reviews[138,139] covering the principles, architecture, and applications of electrochemical biosensors. Here, we present a selection of some of our favourites that exemplify the most common strategies and techniques used in electrochemical biosensing.

Catalytic electrochemical biosensors. Catalytic electrochemical biosensors function on the basis of an interaction between a catalyst (often an enzyme) and a target analyte, which results in a reaction that consumes or produces an electroactive species to be detected at the electrode through change in current[140] or potential.[138] It is important that the reaction occur in close proximity to the electrode surface, as distance can cause signal attenuation.[141] A variety of methods have been used to immobilize enzyme molecules on electrode surfaces, including physical adsorption, covalent attachment, and encapsulation in sol–gel or redox-active polymer layers.[142,143]

Transduction of electrons from soluble redox-active substrates to the electrode can be aided (a) by directly tethering the enzyme's redox core to the electrode surface, or (b) by means of electron transfer mediators. The latter strategy is more flexible and is becoming increasingly popular; common mediators include ferrocene (and derivatives), ferricyanide, methylene blue (MB), benzoquinone, and *N*-methyl phenazine.[138] The phenomenon of diffusion of mediators away from the electrode surface (which reduces the magnitude of signal that can be measured) has led researchers to investigate methods for anchoring both the mediator and enzyme to the electrode. This has been made possible by nanomaterial linkers that can also transport electrons, such as carbon nanotubes and Au nanoparticles. For example, Patolsky *et al.*[144] developed an amperometric glucose sensor that featured glucose oxidase (GOx) tethered to a Au electrode surface *via* single-walled carbon nanotube (SWCNT) mediators. The SWCNTs were terminally functionalized with flavin adenine dinucleotide (FAD) which was attached to apo-glucose oxidase, as illustrated in Fig. 3(a). Zayats *et al.*[145] developed an analogous voltammetric glucose biosensor system using AuNP linker/mediators, which were covalently modified with glucose dehydrogenase (GDH) that was reconstituted around a pyrroloquinoline quinone (PQQ). Oxidation of glucose and electron transfer from the PQQ redox centre to the electrode surface was mediated by the AuNP.

Affinity electrochemical biosensors. The most common biorecognition elements used in affinity electrochemical biosensors are antibodies and nucleic acids that bind with high specificity to their antigens and complementary probes, respectively. A third (emerging) class of electrochemical biosensors use biomimetic probes such as aptamers to detect a diverse range of analytes.

Electrochemical immunosensors & immunoassays. An enormous amount of literature has been produced in the area of electrochemical immunosensors. One should be aware of potentiometric,[146] conductometric,[147] and impedance[148] immunosensors; we limit our discussion here to the most common format: voltammetric sandwich-type immunoassays.

As described in the preceding sections, in sandwich immunoassays, an immobilized primary antibody binds an analyte, which is then bound again by a secondary antibody. When implemented with electrochemical detection, the secondary antibody is typically covalently linked to an enzyme that produces or consumes a redox active species to be detected at the electrode surface. While traditional electrode materials (*e.g.* glassy carbon, Au, *etc.*) are common, alternative materials have recently become popular. For example, Pampalakis and Kelley[149] reported an electrochemical immunosensor in which the primary antibody for prostate specific antigen (PSA) was immobilized on electrodes formed from Au nanowires. Alkaline phosphatase (ALP) covalently attached to a secondary antibody was used to hydrolyze 2-phospho-L-ascorbic acid to ascorbic acid, which in turn reduced Ag^+ ions to Ag metal to be detected by stripping voltammetry. Paper substrates with screen printed electrodes have also been reported for electrochemical ELISAs developed for low-cost applications.[150]

A significant advantage of electrochemical immunoassays implemented in sandwich format is amplification, which enables quantification of trace analytes. While all ELISAs benefit from inherent enzymatic amplification (*i.e.*, one analyte molecule can cause the turnover of many enzyme substrate molecules), electrochemical based ELISAs allow for additional amplification through redox cycling of the electroactive enzyme product. Redox cycling can be done chemically with reductants like NADH[132] or hydrazine,[133] enzymatically (using a second enzyme, different from the secondary-antibody-conjugate[151,152]), or electrochemically[134,135] using interdigitated electrode arrays (IDA). Signal enhancement by as much as 50-fold from redox cycling has been reported.[153]

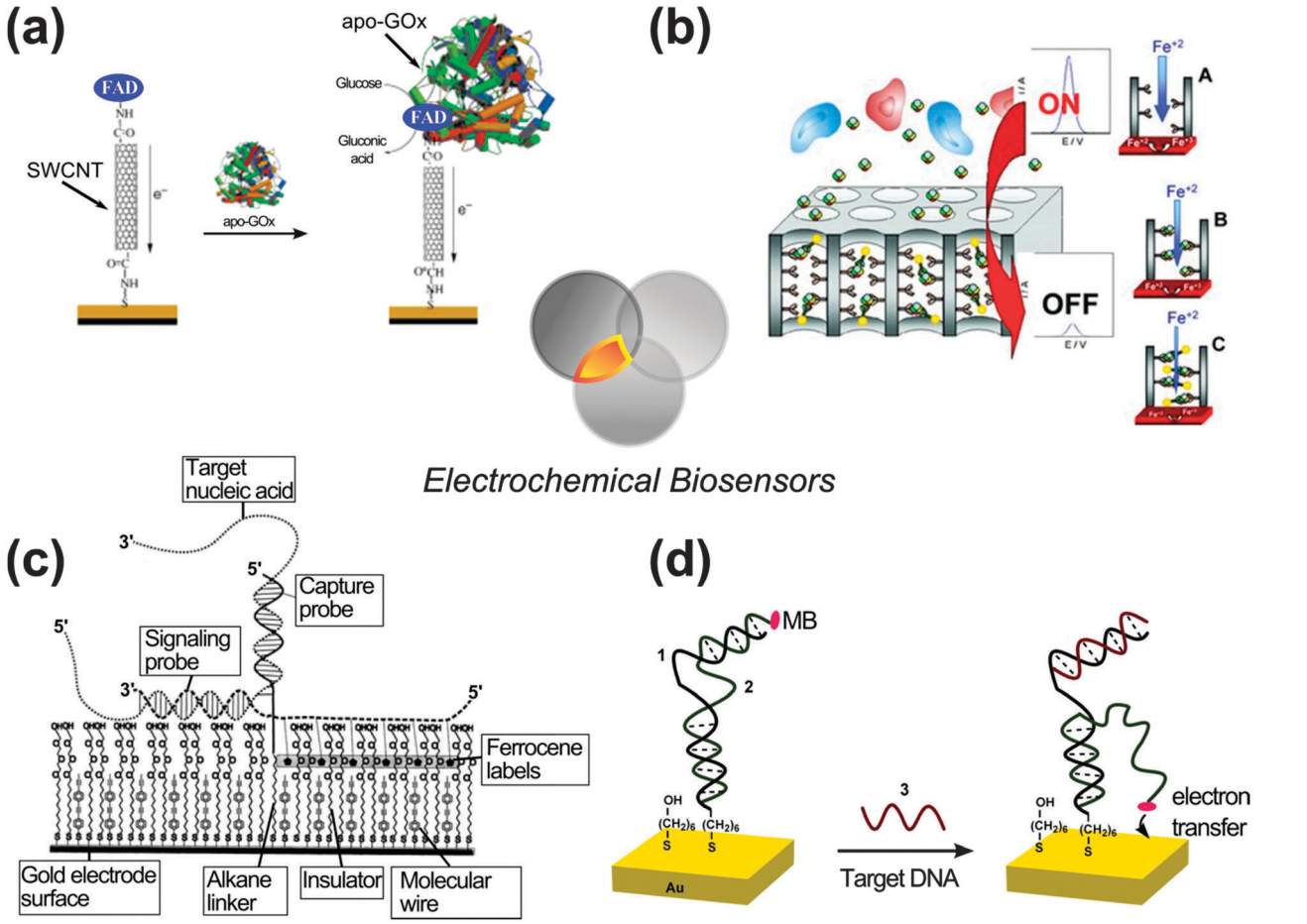

Fig. 3 Electrochemical biosensors. (a) Cartoon sequence (left-to-right) depicting the generation of a catalytic voltammetric biosensor. A layer of SWCNTs is attached to the surface of an electrode, where it is subsequently modified with an enzyme co-factor (FAD), which associates with an enzyme (apo-GOx), which converts glucose to gluconic acid. Each SWCNT acts as an electron mediator, permitting efficient transfer of electrons to the electrode. Reprinted with permission from Patolsky *et al.*,[144] copyright 2004 with permission from Wiley-VCH Verlag GmbH & Co. KGaA. (b) Cartoon depicting a competitive voltammetric immunoassay, in which an electroactive reporter (Fe^{2+}) is blocked from interacting with a WE by the formation of an immunosandwich complex. Additionally, the small dimensions of the nanochannels prevent cells (blue and red) from interfering with the electrode surface. The subset of cartoons, (A–C, right), depicts the growth of the immunosandwich complexes and demonstrates how they physically impede Fe^{2+} transfer to the electrode surface. Reprinted with permission from De La Escosura-Muñiz and Merkoçi,[155] copyright 2011 John Wiley and Sons. (c) Cartoon of a sandwich-type voltammetric biosensor for nucleic acid detection. The capture probe is attached to the electrode surface *via* an alkane linker. Upon binding of target to the immobilized capture probe, a second signaling probe labeled with ferrocene binds to the target. Molecular wires within the SAM transduce the electrons to the electrode surface. Reprinted from Umek *et al.*,[158] copyright 2001 with permission from Elsevier. (d) Cartoon of a "signal-off" E-DNA voltammetric sensor. Binding of complementary DNA (cDNA) to the probe prohibits electron transfer from the ferrocene (Fc) label. Adapted with permission from Fan *et al.*,[159] copyright 2003 National Academy of Sciences, U.S.A.

Immobilizing the recognition layer on the transducer surface is a widely used strategy in electrochemical biosensing. However, immobilization blocks the electrode surface thus limiting the active surface area for an efficient electron transfer. To overcome this phenomenon, Bhimji *et al.*[154] immobilized the recognition element adjacent to the sensing electrode instead of on the surface of the electrode – HIV-1/2 antibodies were immobilized on a planar region near a nanostructured microelectrode (NME). Likewise, De La Escosura-Muñiz and Merkoçi[155,156] reported an immunosensor system with the capture antibody located in nanochannels above the electrode surface as illustrated in Fig. 3(b). Blockage of the nanopores by the immuno-sandwich prevents the redox reporter from accessing the electrode surface, resulting in an "indirect" mode of detection. A similar strategy using electrochemical impedance spectroscopy through porous channels has been reported for the detection of dengue virus particles.[157]

Electrochemical nucleic acid biosensors. The electrochemical detection of DNA was pioneered by Paleček,[160] who studied the redox properties of DNA at a mercury electrode. Since those initial studies, a variety of label-free and labeled sensors for nucleic acids have been developed, typically relying on a complementary probe immobilized on an electrode surface.

One popular sensing technique for nucleic acid biosensors is EIS. These biosensors typically employ a solution-based redox probe such as $[Fe(CN)_6]^{3-/4-}$ or $[Ru(NH_3)_6]^{3+/2+}$ that diffuses through a layer of biorecognition element–analyte complexes to

reach the an electrode surface to carry out the charge transfer process. The charge-transfer resistance, R_{ct}, has been widely used to discern the signal across the range of frequencies before and after biorecognition. EIS has been successfully used for DNA hybridization detection with various target lengths[161] and single nucleotide polymorphisms.[162–164] For example, Cheng *et al.*[165] formed a biorecognition layer composed of DNA probes on AuNPs on an ITO electrode. Dual detection with EIS and localized SPR was possible with this electrode substrate.

Electroactive intercalators, groove binders, and electrostatic reporters have been used in conjunction with voltammetry for nucleic acid biosensors.[166–168] By associating with a double helix, these reporters become preconcentrated at the electrode surface and can be detected by voltammetry. Intercalator surface densities at the electrode surface have been reported on the order of 50 pmol cm^{-2} which limits the absolute electrochemical signal that can be detected. Signals can be improved by the addition of a redox cycling species, such as potassium ferricyanide, which is negatively charged and does not associate with DNA.[166] The reporter is electrochemically reduced and then oxidized by reducing the ferricyanide anion. A large body of work using $Ru(NH_3)_6^{3+}$ as the reporter and $Fe(CN)_6^{3-}$ as the redox cycler has been described by Kelley and co-workers.[169–174] For example, using this electrocatalytic redox cycling strategy in conjunction with NMEs and PNA probes, Lam *et al.*[175] were able to identify bacteria from unpurified lysate in less than 30 min. The use of PNA probes reduces the background signal and increases the sensitivity of detection as the $Ru(NH_3)_6^{3+}$ does not localize to the electrode surface in the presence of PNA alone.

Another strategy is the sandwich assay, which forms the basis of a large selection of electrochemical nucleic acid biosensors. After the target binds an immobilized ''capture'' probe that is shorter in length than the target, a second electroactively labeled ss-DNA ''signaling'' probe that is complementary to another region of the target binds, thus enabling electrochemical detection. For example, Umek *et al.*[158] described a sandwich DNA sensor that relies on a self-assembled monolayer (SAM) consisting of a mixture of DNA–alkanethiol capture probe, molecular wires, and a polyethylene glycol (PEG) terminated alkanethiol spacer/insulator (Fig. 3(c)). The PEG-terminated alkanethiol prevents non-specific adsorption and insulates the electrode surface, minimizing background signal. Upon binding of the target analyte to the immobilized probe, a second probe labeled with ferrocene moieties binds, resulting in an oxidation signal from the molecular wires in the SAM.

Another popular strategy for electrochemical DNA sensing, developed by Plaxco and co-workers,[159] is based on conformation change in the probe after hybridization with the target sequence. Sensors using this strategy, which is similar to FRET-based molecular beacons, are referred to as E-DNA sensors. In the absence of the target, a ferrocene label is kept in proximity to the electrode surface. Hybridization between the oligonucleotide target and probe opens up the hairpin structure and decreases the frequency with which the ferrocene label interacts with the electrode surface resulting in a decrease in voltammetric response. As target concentration increases, the current decreases; this is considered a ''signal-off'' type sensor. In contrast, ''signal-on'' sensors based on a displacement strategy have also been developed, where binding of the target at the distal region of the probe strand releases the redox reporter which can then be oxidized or reduced voltammetrically at the electrode surface.[176] In these sensors, femtomolar detection of the target oligonucleotide is achieved by using a hybridized probe.

Aptamer based electrochemical biosensors. As described in the preceding sections, aptamers are synthetic DNA oligomers with a high binding affinity for a specific, non-nucleic acid analyte. Binding typically causes a change in aptamer conformation which can be detected by variety of approaches, including ''signal-on''[177] and ''signal-off''[178] formats. Recently, Kelley and coworkers[179] developed a so-called ''universal'' strategy relying on displacement of a semi-complementary neutralizer strand, which neutralizes a negatively charged aptamer probe. Binding of the target molecule (protein, DNA, drug *etc.*) displaces the loosely bound neutralizer resulting in an increase in negative charge at the electrode surface, which concentrates the $Ru(NH_3)_6^{3+}$ at the electrode surface that enhances the electrocatalytic cycle resulting in amplified voltammetric signal.

C. Microfluidic biosensing

There is great enthusiasm for the coupling of biosensing and microfluidics, benefitting from the high selectivity of biosensors and the small sample volumes, multiplexing, fast turnaround times, and automation offered by microfluidics. Here we describe representative examples of microfluidic biosensors implemented in microchannels, paper, and DMF formats (excluding electrochemical based biosensors, which are discussed in Section D) for a variety of analytes.

Biosensing in microchannels. There is a large body of literature describing the use of microchannels for biosensing applications, often in formats that allow for multiplexed analysis. For example, Heo and Crooks[180] reported a microchannel-based system for parallel detection of glucose and galactose. Hydrogels with entrapped enzymes for a catalytic fluorescent assay were positioned in a microchannel array. Fluorescence detection mediated by horse-radish peroxidase (HRP) and Amplex Red gave a limit of detection of 0.8 mM for glucose – well below the 4.2–6.4 mM range of normal blood glucose.[181] Another example was reported by Mitsakakis *et al.*,[182] who developed a SAW-based sensor that was addressed in four different regions by a network of microfluidic channels (Fig. 4(a)). The channels were used to functionalize the sensor surface with capture antibodies for four cardiac biomarkers. To enable multianalyte detection on a single sensor, the sample was sequentially added to each channel. The detection limit was 1 nM and the total assay time was less than 30 min. For comparison, clinical assays for the cardiac biomarker C-reactive protein have a detection limit of approximately 0.8–2 nM.[183]

While SAW-based biosensors, requiring only one plane of electrodes, are fairly straightforward to integrate with microchannels,

integration of other mass sensitive transducers such as QCM (which typically require electrodes sandwiching the resonator crystal) in channels – pose a challenge. In one proof-of-concept example, Kato *et al.*[184] integrated a high-frequency QCM with a silicon microchannel for the detection of human IgG. Encapsulating a quartz resonator within a microchannel reduced its fragility; metal electrodes were not needed, reducing the thickness of the crystal thus increasing the resonant frequency of the system. The authors demonstrated the detection of 6 μg mL^{-1} of human IgG in pure water using this sensor system.

For nucleic acid detection, multiple microchannels are useful for spatial multiplexing and also for eliminating cross-contamination between sensors or sensor regions. However, it is also possible to multiplex within a single microchannel; for example, Peng *et al.*[185] developed a sensitive nucleic acid microfluidic biosensor on the basis of fluorescence quenching by Ag nanoparticles. DNA probes with terminal fluorescent labels were covalently attached to an Ag nanoparticle modified glass surface. A microarray printer was used to spot DNA probes onto the surface, which was then enclosed by annealing within

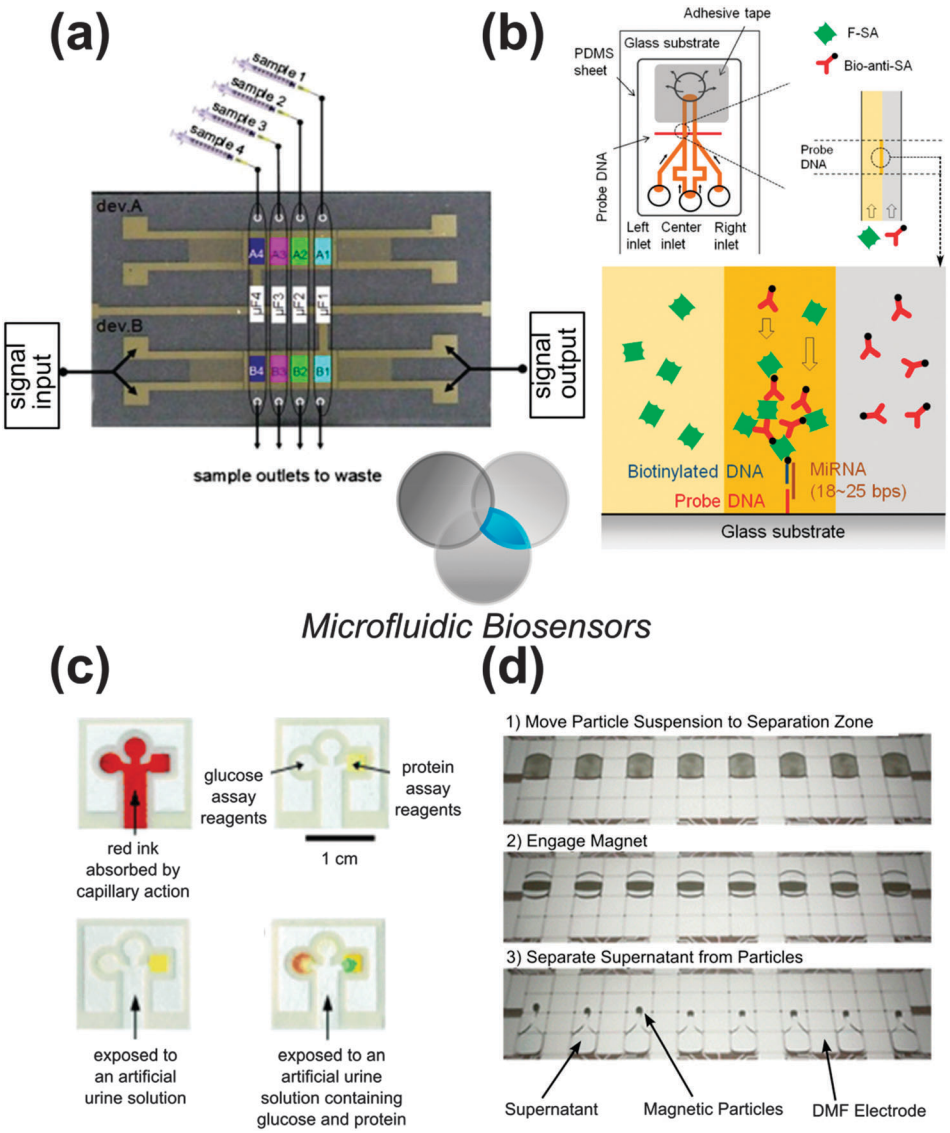

Fig. 4 Microfluidic biosensors. (a) Illustration of a SAW biosensor with parallel microfluidic channels. Electrical contacts are available for signal input and output. The single sensor is capable of measuring four different samples. Reprinted from Mitsakakis and Gizeli,[182] copyright 2011 with permission from Elsevier. (b) Cartoon of a microfluidic device (top left) and mechanism of LFDA (top right and below). The probe-micro RNA-biotinylated DNA sandwich starts the formation of the streptavidin–biotin dendrimer complex. Laminar flow enables the continual addition of fluorescent streptavidin (green) and biotinylated anti-streptavidin antibodies (red). Reprinted from Arata *et al.*[187] under Creative Commons license attribution. (c) Photographs of a paper microfluidic device used for the determination of glucose and protein. Hydrophobic patterning directs the flow of liquids by capillary action. The devices have two regions, one for a glucose assay and another for a protein assay. Reprinted with permission from Martinez *et al.*,[63] copyright 2007 Wiley-VCH Verlag GmbH & Co. KGaA. (d) Video stills of magnetic bead separations on DMF. Engaging a permanent magnet allows the supernatant to be separated from the magnetic particles. Parallel processing of multiple samples can be implemented on large arrays of DMF electrodes. Adapted with permission from Choi *et al.*,[99] copyright 2013 American Chemical Society.

a microchannel. The flow in the channel was useful for allowing fast response times – without flow, incubation overnight is necessary for low concentration detection but with flow, detection times were decreased to as little as six minutes. With this microfluidic biosensor, reagent consumption is significantly reduced, requiring sample volumes of only 4 μL. Another example of multiplexing by microfluidics for nucleic acid detection was reported by Lechuga *et al.*[186] In this work, 20 micromechanical cantilever sensors were integrated with microchannels to enable straightforward sample delivery. The authors also reported that individual sensors can be addressed by using individual channels.

Beyond multiplexing and handling small sample volumes, physical properties inherent to microfluidics can be used to enhance the capabilities of biosensors. For example, laminar flow in low-Re conditions can be used to enhance signal amplification for the detection of micro RNA.[187] Laminar flow-assisted dendritic amplification (LFDA) is a technique whereby two amplification reagents are simultaneously supplied and confined to a detection zone by means of laminar flow, as depicted in Fig. 4(b). The amplification reagents are fluorescently labeled streptavidin and biotinylated anti-streptavidin which bind the surface-captured micro RNA target. Their continual addition propagates a dendritic structure resulting in lower detection limits, which are crucial as micro RNA concentrations in tissues are on the order of 1–10 pM.[188]

Paper-based biosensing. Paper-based biosensors are a straightforward route to selective, low-cost diagnostics. For example, Martinez *et al.*[63] presented a qualitative colourimetric assay for glucose and protein. The device (Fig. 4(c)) split the sample into two regions for parallel testing and colourimetric results could be compared to artificial standards. More complicated assays such as ELISA are a challenge to implement with paper because of the need for multiple steps (*i.e.* sample delivery, washing steps, and antibody delivery). For ideal end-user operation, a single step is preferable – sample introduction. One such single-step paper-based immunoassay was developed by Apilux *et al.*[189] To overcome the challenge of timing reagent delivery, channels of varying lengths were patterned on nitrocellulose paper using an inkjet printer and dipropylene glycol methyl ether acetate "ink." This allowed reagents to be delivered to test sites at the appropriate times and only required a sample introduction step. Quantitative results for the detection of human chorionic gonadotropin (hCG) were determined by photographing the paper immunosensor and analyzing the intensities of various colour channels. The paper immunosensor had a limit of detection as low as 0.81 ng mL^{-1}, which is 2–12 times lower than the detectable levels of hCG determined by commercial pregnancy strips.

DMF-based biosensing. For complex bioassays, DMF is a useful microfluidic format because of its configurability and flexible control. Heterogeneous immunoassays making use of magnetic particles are a popular choice for conducting immunoassays on DMF. Early reports of DMF-based immunoassays used a permanent magnet in a fixed region and aqueous droplets surrounded by silicone oil.[98] ELISAs for interlukin-6 and insulin were demonstrated, and a chemiluminescent signal was detected from the catalyzed activity of alkaline phosphatase conjugated reporter antibodies. IgE immunoassays using fluorescently labeled IgE aptamers have also been performed on magnetic nanoparticles.[190] Ng *et al.*[96] presented the first DMF particle-based immunoassay without the need for an oil carrier fluid. The same group also incorporated motorized magnets[99] into a shoebox-sized instrument, and recently demonstrated its efficacy for screening a panel of patient samples to diagnose rubella immunity.[100] Fig. 4(d) demonstrates how this instrument can be used to separate multiple aliquots of magnetic particles from supernatant.

The DMF format can also be used to enhance nucleic acid biosensor performance. Malic *et al.*[191] coupled an SPRi based nucleic acid sensor with DMF. In this report, DMF offered two advantages: (1) the ability to address independent spots with droplets, making hybridization detection flexible and reconfigurable, and (2) the use of the DMF architecture to apply electric fields to enhance probe deposition. The authors reported that a negative DC voltage led to a build-up of positive charge on the substrate, which in turn, increased the probe density of negatively charged DNA.

D. Microfluidic electrochemical biosensing

Microfluidic electrochemical biosensing is a new application area that is emerging from the convergence of the three sub-fields of electrochemistry, biosensing, and microfluidics. We propose that microfluidic electrochemical biosensors may be particularly fertile ground for the development of the next generation of portable analysis systems, whether they are applied to disease diagnostics, to cell culture and analysis, or to many other applications. Examples listed here are categorized in terms of microfluidic format, with a final section describing commercially available systems (of various formats).

Microchannel-based electrochemical biosensing. The microchannel format confers numerous analytical advantages (and also some disadvantages) for electrochemical biosensing. As an example of the former, the confinement of electroactive species near the detector in a small volume in a microchannel allows significant improvements in sensitivity, allowing for amperometric detection of DNA in an enzyme-linked hybridization assay at the 100 pM level.[192] As an example of the latter, Lamberti *et al.*[193] studied the effect of flow on indirect catalytic electrochemical biosensors using a simple GOx based system. Oxidation of glucose by immobilized GOx in a microchannel yielded gluconic acid and H_2O_2, which was detected electrochemically. Results of this study showed that flow-rate is a critical parameter for biosensor performance and must be optimized to prevent the washing away of electron transfer mediators and electroactive products. For the most part, however, the microchannel format has become increasingly popular for electrochemical biosensing because of numerous structural advantages, including improvements in throughput, integration, portability, and analysis time.

Microfluidic electrochemical biosensors are particularly useful for improving throughput, which is important for applications in

which multiple samples must be analyzed quickly. For example, Wisitsoraat *et al.*[194] and Ruecha *et al.*[195] reported the development of microfluidic chips bearing amperometric biosensors for cholesterol relying on cholesterol oxidase (ChOx), both with throughput of 60 samples per h. In the former report, ChOx was immobilized on a CNT WE within a microfluidic flow injection system. In the latter report, the ChOx element was decoupled from the sensing electrode and introduced in the running buffer of a capillary electrophoresis setup. The reaction between cholesterol and ChOx produces H_2O_2, which was detected by a Au WE.

Microfluidic electrochemical biosensors are also particularly useful for integration of cell culture with analysis. For example, voltammetric and amperometric biosensors for H_2O_2 generated by cellular activities using HRP have been incorporated into microfluidic systems.[196] Yan *et al.*[197] and Matharu *et al.*[198] used HRP trapped in polyethylene glycol (PEG) hydrogels positioned over Au electrodes. Both reports used the same device architecture, which is illustrated in Fig. 5(a). Yan *et al.*[197] detected H_2O_2 release from activated macrophages cultured in the microfluidic chip while Matharu *et al.*[198] probed the effects of ethanol and antioxidants by studying reactive oxide species produced in hepatocytes cultured in the device.

Microchannels are also useful for making electrochemical biosensing assays portable. Itoh *et al.*[199] presented a droplet-based microfluidic system for the rapid determination of fish freshness, monitored as a function of adenosine triphosphate (ATP) concentration. ATP can be detected electrochemically by means of the enzymes glycerol kinase (GK) and glycerol-3-phosphate oxidase (G3PO) with glycerol. The phosphorylation of glycerol to glycerol-3-phosphate by GK requires a stoichiometric amount of ATP. Oxidation of glycerol-3-phosphate by G3PO produces H_2O_2, which can be quantified electrochemically. The authors demonstrated a good correlation between their microfluidic results and those generated by conventional HPLC.

Implementation in microchannels makes electrochemical biosensing fast. For example, Messina *et al.*[200] developed an immunosensor system in which primary antibodies for interleukin-6 (IL-6) were immobilized on packed glass beads contained within a central PMMA microchannel. Working, reference, and CEs were positioned downstream of the packed beads in secondary cross channels. The authors reported that for sample sizes of 100 μL, flow rates above 6 μL min^{-1} resulted in a decrease in amperometric signal. The total assay time was approximately 25 min. In another example, a microfluidic immunoassay for cholera toxin subunit B was developed in which antibodies were conjugated to liposomes containing ferri/ferrocyanide.[201] Lysis of the liposomes released ferri/ferrocyanide which could be detected downstream by amperometry. Microfluidic channels were used to deliver the sample and the lysis detergent and paramagnetic particles were used as a support for the capture antibodies. The turnaround time for the assay was 1 h, significantly faster relative to comparable techniques.

In some of the early reports describing the integration of microfluidics with electrochemical biosensors, the microfluidic device architecture was primitive, incorporating only one or a few microchannels. These designs can complicate the loading of multiple reagents through a single input valve; to overcome this challenge, Kellner *et al.*[202] reported a device in which multiple reagents were controlled using a syringe pump and a 9-port valve. The device, pictured in Fig. 5(b), contains all the necessary reagents on-chip for performing an amperometric ELISA for either CEA or cancer antigen 15-3.

There are many other reports of microchannel-based electrochemical biosensing. Space precludes listing them all; we include a few interesting (and unique) examples here. Berdat *et al.*[203] reported the detection of 1 nM DNA using an IDA in a microfluidic channel. DNA probes were immobilized between the interdigitated electrodes and hybridization with complementary targets results in an increase in conductance, which could be calculated from the charge-transfer resistance as determined by EIS measurements. In this report, the measurements were taken in de-ionized H_2O and no labels or reporters were necessary. For robust environmental sensing, Lin *et al.*[204] implemented label-free detection of an arbitrary DNA oligonucleotide using an organic electrochemical transistor in a flexible microfluidic device, pictured in Fig. 5(c). Hybridization of target DNA was enhanced by pulsing a small positive potential at the sensing electrodes which extends the detection limit to 10 pM. Swensen *et al.*[205] reported an aptamer based system for the real-time detection of cocaine within a microfluidic channel. Sensor surfaces can be regenerated by flowing a blank sample[205] or exposure to urea.[206] The ability to measure analyte concentrations in real-time is particularly useful for cell culture studies. For example, numerous methods have been developed to detect cell secretion of signaling molecules, including tumor necrosis factor-α,[206,207] interferon-γ,[206] and transforming growth factor-β.[208] Kim *et al.*[209] incorporated electrodes with a centrifugal microfluidic disc for the amperometric detection of C-reactive protein by a sandwich immunoassay on polystyrene beads. Coupling with the disc-format showed a 5-fold in improvement in the detection limit over a similar stationary assay.

Paper-based electrochemical biosensing. The (modern renaissance of the) "paper microfluidic" format is still quite new, and there are only a few examples of integrated paper-based electrochemical biosensors. Despite this, we propose that this is a particularly promising strategy for portable analysis, given the combination of miniaturized detection with straightforward incorporation of dried reagents. For example, Zhao *et al.*[210] developed a paper-based microfluidic cartridge coupled to a low-cost potentiostat for the determination of glucose, lactate, and uric acid. All reagents including $K_3Fe(CN)_6$ and oxidase enzymes were stored in dry form within the paper device. As shown in Fig. 5(d), the device consists of a sample inlet and screen printed electrodes over the test zone, which was directly integrated with a potentiostat *via* metal clamps and Ag connections. Multiplexing circuitry was added to the USB controlled potentiostat to enable detection at all eight test spots. This low-cost device was shown to have detection limits for all three analytes within the appropriate clinically relevant ranges and to

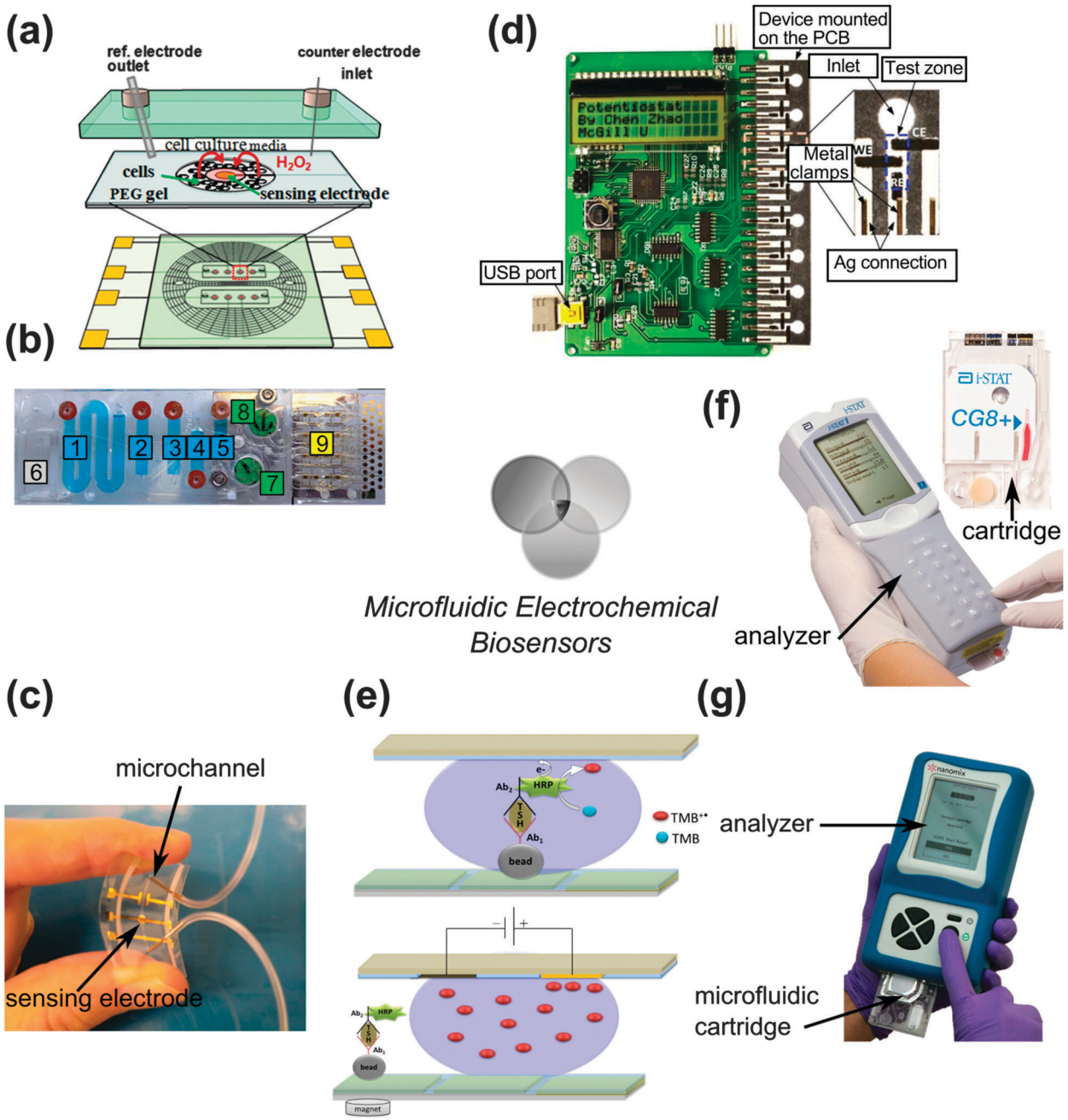

Fig. 5 Microfluidic electrochemical biosensors. (a) Schematic of a microfluidic device for real-time electrochemical monitoring of cells grown in a PEG hydrogel matrix. Reprinted with permission from Yan *et al.*,[197] copyright 2011 AIP Publishing. (b) Photograph of a computer controlled channel-based system with reagent storage (1–5), on-chip valves (7 & 8) and electrochemical sensing area (9). Adapted with permission from Kellner *et al.*,[202] copyright 2011 Wiley-VCH Verlag GmbH & Co. KGaA. (c) Photograph of a flexible microfluidic channel-based device for nucleic acid detection. Reprinted with permission from Lin *et al.*,[204] copyright 2011 Wiley-VCH Verlag GmbH & Co. KGaA. (d) Photograph of a paper-fluidic device incorporated onto a low-cost potentiostat. The test strips wick the sample into a detection zone with a three electrode setup. Adapted from Zhao *et al.*[210] under Creative Commons license attribution. (e) Cartoon of an electrochemical immunoassay implemented in a DMF device. The immune-sandwich is prepared on a magnetic bead and HRP converts the substrate TMB to TMB^+. Droplet movement separates the enzyme product from the magnetic particles and delivers the product to electrodes on the top plate for detection. Adapted from the methods described by Shamsi *et al.*[97] (f) Photograph of the Abbott Point of Care i-STAT®, the leading commercial microfluidic electrochemical-detection based point of care system. The handheld analyzer is compatible with a variety of microfluidic cartridges (inset). Reprinted with permission from Abbott Laboratories, Abbott Park, IL. (g) Photograph of the Nanōmix eLab, a cartridge based hand-held microfluidic electrochemical biosensor currently available for research purposes. Reprinted with permission from Nanōmix. Emeryville, CA.

outperform comparable commercial biosensors. Specifically, the reported limit of detection for glucose was 0.35 mM, compared to 0.83 mM for commercial glucose meters.

DMF-based electrochemical biosensing. DMF is also relatively new, and there are few examples of the application of this technology to electrochemical biosensing. Despite this, we propose

that DMF is particularly well-suited for coupling complex sample handling regimens with electrochemical biosensors. For example, Shamsi *et al.*[97] reported an amperometric ELISA using paramagnetic particles and electrodes incorporated with a DMF chip (Fig. 5(e)). The electrode layout of the DMF device made it possible to implement an eight-step protocol including sample and reagent loading steps, multiple supernatant/particle separation steps, and multiple particle-washing steps. Thyroid stimulating hormone (TSH) was detected by means of a sandwich assay with a secondary antibody conjugated to HRP. Turnover of 3,3′,5,5′-tetramethylbenzidine (TMB) to TMB^+ by HRP was detected by amperometry at an Au plated ITO electrode.

Commercial microfluidic electrochemical biosensing. The microfluidic electrochemical biosensor is an idea whose time has come, and numerous versions of such devices have been commercialized for portable, point-of-care analysis. The largest market of such devices is likely the personal blood glucose meter, with an estimated worldwide value near $10 billion.[211] Many of these meters rely on wicking blood through short microchannels or paper substrates. Perhaps the best-known example of a system that embodies many of the attributes described in this review is the Abbott Point of Care i-STAT® System (Fig. 5(f)). The analyzer is designed to be used with one of several cartridges that contain enclosed microchannels designed to process small whole blood volumes: 17 to 95 μL depending on the cartridge type. More than 50 million such cartridges are produced each year at the Abbott Point of Care manufacturing facility located in Ottawa, Ontario. The cartridges enable quantitation of 25 different analytes and blood chemistry parameters; all of the detection is electrochemical, and many of the assays rely on catalytic biosensors (*e.g.* urea nitrogen, glucose, creatinine, lactate, ACT Celite, ACT Kaolin, and PT/INR), ion selective electrodes (*e.g.* Na^+, K^+, iCa^{2+}) or affinity biosensors (cTnI, creatine kinase-MB, and B-type natriuretic peptide).[212] Apart from the i-STAT, other microfluidic electrochemical point-of-care devices have been developed, but do not (yet) have the appropriate clearance for diagnostic use. For example, the Nanōmix eLab (Fig. 5(g)) is a similar hand-held, cartridge based device for the detection of cardiac biomarkers.[213] Other point-of-care devices based on electrochemical biosensors are also being pursued, including an instrument for HIV diagnostics called the Daktari CD4,[214] as well as the GeneFluidics bench-top system for electrochemical immunoassays and nucleic acid assays.[215]

Conclusion and a look to the future

The intersection of electrochemistry, biosensors, and microfluidics is pushing the frontiers of the traditional disciplines in science and engineering. This review covers each of these areas and their overlaps, with an emphasis on applications. Most of the examples described here are used for applications in biology and medicine, but we propose that opportunities abound for related methods in environmental sensing and monitoring as well as the agriculture and veterinary sectors. Further, while there are many examples of microfluidic electrochemical biosensors for nucleic acids, proteins, and antibodies, there seems to be an opportunity for new methods capable of quantifying small molecules (suggesting a role for aptamer-based sensors). Along with these opportunities, microfluidic electrochemical biosensors face competition as other techniques decrease in cost and size. For example, bench-top and personal mass spectrometers are available – eliminating the need for biorecognition elements in order to achieve highly specific detection. Yet, in the face of this competition, advancements in microfluidic electrochemical biosensors may lead to supplementary and even complementary technologies. We propose, based on the trajectory of advances to date, that the overlapping areas of microfluidics, electrochemistry, and biosensors will continue to evolve in unpredictable directions. It will be exciting to see what new ideas emerge from this development – we predict that the outcome will be interesting and potentially important for the world that we live in.

References

1 A. J. Bard and L. R. Faulkner, *Electrochemical Methods: Fundamentals and Applications*, John Wiley & Sons Inc., USA, 2nd edn, 2000.
2 W. Schmickler and E. Santos, *Interfacial Electrochemistry*, Oxford University Press, New York, 2nd edn, 2010.
3 D. G. Buerk, *Biosensors Theory and Applications*, Technomic Publishers, USA, 1993.
4 V. Perumal and U. Hashim, *J. Appl. Biomed.*, 2014, **12**, 1–15.
5 J. Kirsch, C. Siltanen, Q. Zhou, A. Revzin and A. Simonian, *Chem. Soc. Rev.*, 2013, **42**, 8733–8768.
6 J. Puigmarti-Luis, *Chem. Soc. Rev.*, 2014, **43**, 2253–2271.
7 K. Choi, A. H. C. Ng, R. Fobel and A. R. Wheeler, *Annu. Rev. Anal. Chem.*, 2012, **5**, 413–440.
8 D. Mark, S. Haeberle, G. Roth, F. von Stetten and R. Zengerle, *Chem. Soc. Rev.*, 2010, **39**, 1153–1182.
9 F. K. Balagaddé, L. You, C. L. Hansen, F. H. Arnold and S. R. Quake, *Science*, 2005, **309**, 137–140.
10 A. W. Martinez, S. T. Phillips and G. M. Whitesides, *Proc. Natl. Acad. Sci. U. S. A.*, 2008, **105**, 19606–19611.
11 C. P. Andrieux, P. Hapiot and J. M. Saveant, *Chem. Rev.*, 1990, **90**, 723–738.
12 W. Xiao and D. Wang, *Chem. Soc. Rev.*, 2014, **43**, 3215–3228.
13 A. Adriaens and M. Dowsett, *Acc. Chem. Res.*, 2010, **43**, 927–935.
14 M. T. Mayer, Y. Lin, G. Yuan and D. Wang, *Acc. Chem. Res.*, 2013, **46**, 1558–1566.
15 Y. Xiang, S. Lu and S. P. Jiang, *Chem. Soc. Rev.*, 2012, **41**, 7291–7321.
16 Z. G. Arias, J. L. Muñiz Álvarez and J. M. López Fonseca, *Electroanalysis*, 2004, **16**, 1044–1050.
17 J. Wang and M. Musameh, *Anal. Lett.*, 2003, **36**, 2041–2048.
18 B.-Y. Chang and S.-M. Park, *Annu. Rev. Anal. Chem.*, 2010, **3**, 207–229.
19 D. R. Theavenot, K. Toth, R. A. Durst and G. S. Wilson, *Pure Appl. Chem.*, 1999, **71**, 2333–2348.

20 S. M. Borisov and O. S. Wolfbeis, *Chem. Rev.*, 2008, **108**, 423–461.
21 J. Newman and S. Setford, *Mol. Biotechnol.*, 2006, **32**, 249–268.
22 A. Sassolas, B. D. Leca-Bouvier and L. J. Blum, *Chem. Rev.*, 2008, **108**, 109–139.
23 A. D. Ellington and J. W. Szostak, *Nature*, 1992, **355**, 850–852.
24 T. Hianik and J. Wang, *Electroanalysis*, 2009, **21**, 1223–1235.
25 S. M. Knudsen and A. D. Ellington, in *The Aptamer Handbook*, ed. S. Klussmann, Wiley-VCH Verlag GmbH & Co. KGaA, Weinheim, 2006, ch. 13, pp. 290–310.
26 Y. Wang, C. Li, X. Li, Y. Li and H.-B. Kraatz, *Anal. Chem.*, 2008, **80**, 2255–2260.
27 X. Guo, *J. Biophotonics*, 2012, **5**, 483–501.
28 S. Scaranoa, M. Mascini, A. P. F. Turner and M. Minunni, *Biosens. Bioelectron.*, 2010, **25**, 957–966.
29 J. Breault-Turcot and J.-F. Masson, *Anal. Bioanal. Chem.*, 2012, **403**, 1477–1484.
30 G. Steiner, *Anal. Bioanal. Chem.*, 2004, **379**, 328–331.
31 K. Länge, B. Rapp and M. Rapp, *Anal. Bioanal. Chem.*, 2008, **391**, 1509–1519.
32 C. K. O'Sullivan and G. G. Guilbault, *Biosens. Bioelectron.*, 1999, **14**, 663–670.
33 J. Fritz, M. K. Baller, H. P. Lang, H. Rothuizen, P. Vettiger, E. Meyer, H.-J. Güntherodt, C. Gerber and J. K. Gimzewski, *Science*, 2000, **288**, 316–318.
34 G. M. Whitesides, *Nature*, 2006, **442**, 368–373.
35 A. Manz, N. Graber and H. M. Widmer, *Sens. Actuators, B*, 1990, **1**, 244–248.
36 D. J. Harrison, A. Manz, Z. Fan, H. Luedi and H. M. Widmer, *Anal. Chem.*, 1992, **64**, 1926–1932.
37 A. R. Wu, N. F. Neff, T. Kalisky, P. Dalerba, B. Treutlein, M. E. Rothenberg, F. M. Mburu, G. L. Mantalas, S. Sim, M. F. Clarke and S. R. Quake, *Nat. Methods*, 2014, **11**, 41–46.
38 J. Baek, P. M. Allen, M. G. Bawendi and K. F. Jensen, *Angew. Chem., Int. Ed.*, 2011, **50**, 627–630.
39 I. R. Baxendale, S. V. Ley, C. D. Smith and G. K. Tranmer, *Chem. Commun.*, 2006, 4835–4837.
40 S. H. Tan, F. Maes, B. Semin, J. Vrignon and J.-C. Baret, *Sci. Rep.*, 2014, **4**, 4787.
41 M. J. Fuerstman, P. Deschatelets, R. Kane, A. Schwartz, P. J. A. Kenis, J. M. Deutch and G. M. Whitesides, *Langmuir*, 2003, **19**, 4714–4722.
42 J. Qin and A. R. Wheeler, *Lab Chip*, 2007, **7**, 186–192.
43 A. Manz, D. J. Harrison, E. M. J. Verpoorte, J. C. Fettinger, A. Paulus, H. Lüdi and H. M. Widmer, *J. Chromatogr. A*, 1992, **593**, 253–258.
44 D. J. Beebe, G. A. Mensing and G. M. Walker, *Annu. Rev. Biomed. Eng.*, 2002, **4**, 261–286.
45 T. M. Squires and S. R. Quake, *Rev. Mod. Phys.*, 2005, **77**, 977–1026.
46 B. J. Kirby, *Micro- and Nanoscale Fluid Mechanics: Transport in Microfluidic Devices*, Cambridge University Press, New York, 2010.
47 P. Tabeling, *Introduction to Microfluidics*, Oxford University Press, New York, 2010.
48 W. Du, L. Li, K. P. Nichols and R. F. Ismagilov, *Lab Chip*, 2009, **9**, 2286–2292.
49 S. C. Jacobson, A. W. Moore and J. M. Ramsey, *Anal. Chem.*, 1995, **67**, 2059–2063.
50 R. Gorkin, J. Park, J. Siegrist, M. Amasia, B. S. Lee, J.-M. Park, J. Kim, H. Kim, M. Madou and Y.-K. Cho, *Lab Chip*, 2010, **10**, 1758–1773.
51 S. R. Quake and A. Scherer, *Science*, 2000, **290**, 1536–1540.
52 K. Ren, J. Zhou and H. Wu, *Acc. Chem. Res.*, 2013, **46**, 2396–2406.
53 S. K. W. Dertinger, D. T. Chiu, N. L. Jeon and G. M. Whitesides, *Anal. Chem.*, 2001, **73**, 1240–1246.
54 N. Li Jeon, H. Baskaran, S. K. W. Dertinger, G. M. Whitesides, L. Van De Water and M. Toner, *Nat. Biotechnol.*, 2002, **20**, 826–830.
55 S.-Y. Teh, R. Lin, L.-H. Hung and A. P. Lee, *Lab Chip*, 2008, **8**, 198–220.
56 A. B. Theberge, F. Courtois, Y. Schaerli, M. Fischlechner, C. Abell, F. Hollfelder and W. T. S. Huck, *Angew. Chem., Int. Ed.*, 2010, **49**, 5846–5868.
57 A. Huebner, S. Sharma, M. Srisa-Art, F. Hollfelder, J. B. Edel and A. J. deMello, *Lab Chip*, 2008, **8**, 1244–1254.
58 J. J. Agresti, E. Antipov, A. R. Abate, K. Ahn, A. C. Rowat, J.-C. Baret, M. Marquez, A. M. Klibanov, A. D. Griffiths and D. A. Weitz, *Proc. Natl. Acad. Sci. U. S. A.*, 2010, **107**, 4004–4009.
59 J.-C. Baret, O. J. Miller, V. Taly, M. Ryckelynck, A. El-Harrak, L. Frenz, C. Rick, M. L. Samuels, J. B. Hutchison, J. J. Agresti, D. R. Link, D. A. Weitz and A. D. Griffiths, *Lab Chip*, 2009, **9**, 1850–1858.
60 A. R. Abate, T. Hung, P. Mary, J. J. Agresti and D. A. Weitz, *Proc. Natl. Acad. Sci. U. S. A.*, 2010, **107**, 19163–19166.
61 X. Niu, F. Gielen, J. B. Edel and A. J. deMello, *Nat. Chem.*, 2011, **3**, 437–442.
62 B. J. Hindson, K. D. Ness, D. A. Masquelier, P. Belgrader, N. J. Heredia, A. J. Makarewicz, I. J. Bright, M. Y. Lucero, A. L. Hiddessen, T. C. Legler, T. K. Kitano, M. R. Hodel, J. F. Petersen, P. W. Wyatt, E. R. Steenblock, P. H. Shah, L. J. Bousse, C. B. Troup, J. C. Mellen, D. K. Wittmann, N. G. Erndt, T. H. Cauley, R. T. Koehler, A. P. So, S. Dube, K. A. Rose, L. Montesclaros, S. Wang, D. P. Stumbo, S. P. Hodges, S. Romine, F. P. Milanovich, H. E. White, J. F. Regan, G. A. Karlin-Neumann, C. M. Hindson, S. Saxonov and B. W. Colston, *Anal. Chem.*, 2011, **83**, 8604–8610.
63 A. W. Martinez, S. T. Phillips, M. J. Butte and G. M. Whitesides, *Angew. Chem., Int. Ed.*, 2007, **46**, 1318–1320.
64 R. H. Müller and D. L. Clegg, *Anal. Chem.*, 1949, **21**, 1123–1125.
65 E. Carrilho, A. W. Martinez and G. M. Whitesides, *Anal. Chem.*, 2009, **81**, 7091–7095.
66 K. Abe, K. Suzuki and D. Citterio, *Anal. Chem.*, 2008, **80**, 6928–6934.
67 A. W. Martinez, S. T. Phillips, B. J. Wiley, M. Gupta and G. M. Whitesides, *Lab Chip*, 2008, **8**, 2146–2150.

68 J. Olkkonen, K. Lehtinen and T. Erho, *Anal. Chem.*, 2010, **82**, 10246–10250.
69 X. Li, D. R. Ballerini and W. Shen, *Biomicrofluidics*, 2012, **6**, 011301.
70 B. R. Lutz, P. Trinh, C. Ball, E. Fu and P. Yager, *Lab Chip*, 2011, **11**, 4274–4278.
71 A. K. Yetisen, M. S. Akram and C. R. Lowe, *Lab Chip*, 2013, **13**, 2210–2251.
72 P. Yager, T. Edwards, E. Fu, K. Helton, K. Nelson, M. R. Tam and B. H. Weigl, *Nature*, 2006, **442**, 412–418.
73 J. Hu, S. Wang, L. Wang, F. Li, B. Pingguan-Murphy, T. J. Lu and F. Xu, *Biosens. Bioelectron.*, 2014, **54**, 585–597.
74 Z. Nie, C. A. Nijhuis, J. Gong, X. Chen, A. Kumachev, A. W. Martinez, M. Narovlyansky and G. M. Whitesides, *Lab Chip*, 2010, **10**, 477–483.
75 S. Wang, L. Ge, X. Song, J. Yu, S. Ge, J. Huang and F. Zeng, *Biosens. Bioelectron.*, 2012, **31**, 212–218.
76 J. L. Delaney, C. F. Hogan, J. Tian and W. Shen, *Anal. Chem.*, 2011, **83**, 1300–1306.
77 B. Liu, D. Du, X. Hua, X.-Y. Yu and Y. Lin, *Electroanalysis*, 2014, **26**, 1214–1223.
78 M. J. Jebrail, M. S. Bartsch and K. D. Patel, *Lab Chip*, 2012, **12**, 2452–2463.
79 A. R. Wheeler, *Science*, 2008, **322**, 539–540.
80 R. B. Fair, *Microfluid. Nanofluid.*, 2007, **3**, 245–281.
81 J. Lee, H. Moon, J. Fowler, T. Schoellhammer and C.-J. Kim, *Sens. Actuators, A*, 2002, **95**, 259–268.
82 T. B. Jones, *Langmuir*, 2002, **18**, 4437–4443.
83 D. Chatterjee, H. Shepherd and R. L. Garrell, *Lab Chip*, 2009, **9**, 1219–1229.
84 R. Fobel, A. E. Kirby, A. H. C. Ng, R. R. Farnood and A. R. Wheeler, *Adv. Mater.*, 2014, **26**, 2838–2843.
85 H. Ko, J. Lee, Y. Kim, B. Lee, C.-H. Jung, J.-H. Choi, O.-S. Kwon and K. Shin, *Adv. Mater.*, 2014, **26**, 2335–2340.
86 R. Fobel, C. Fobel and A. R. Wheeler, *Appl. Phys. Lett.*, 2013, **102**, 193513.
87 Z. Long, A. M. Shetty, M. J. Solomon and R. G. Larson, *Lab Chip*, 2009, **9**, 1567–1575.
88 S.-Y. Park, M. A. Teitell and E. P. Y. Chiou, *Lab Chip*, 2010, **10**, 1655–1661.
89 Y. Q. Fu, J. K. Luo, X. Y. Du, A. J. Flewitt, Y. Li, G. H. Markx, A. J. Walton and W. I. Milne, *Sens. Actuators, B*, 2010, **143**, 606–619.
90 A. A. Darhuber, J. P. Valentino and S. M. Troian, *Lab Chip*, 2010, **10**, 1061–1071.
91 B. Hadwen, G. R. Broder, D. Morganti, A. Jacobs, C. Brown, J. R. Hector, Y. Kubota and H. Morgan, *Lab Chip*, 2012, **12**, 3305–3313.
92 N. A. Mousa, M. J. Jebrail, H. Yang, M. Abdelgawad, P. Metalnikov, J. Chen, A. R. Wheeler and R. F. Casper, *Sci. Transl. Med.*, 2009, **1**, 1ra2.
93 M. J. Jebrail, H. Yang, J. M. Mudrik, N. M. Lafreniere, C. McRoberts, O. Y. Al-Dirbashi, L. Fisher, P. Chakraborty and A. R. Wheeler, *Lab Chip*, 2011, **11**, 3218–3224.
94 I. A. Eydelnant, B. Betty Li and A. R. Wheeler, *Nat. Commun.*, 2014, **5**, 3355.
95 H. Yang, J. M. Mudrik, M. J. Jebrail and A. R. Wheeler, *Anal. Chem.*, 2011, **83**, 3824–3830.
96 A. H. C. Ng, K. Choi, R. P. Luoma, J. M. Robinson and A. R. Wheeler, *Anal. Chem.*, 2012, **84**, 8805–8812.
97 M. H. Shamsi, K. Choi, A. H. C. Ng and A. R. Wheeler, *Lab Chip*, 2014, **14**, 547–554.
98 R. S. Sista, A. E. Eckhardt, V. Srinivasan, M. G. Pollack, S. Palanki and V. K. Pamula, *Lab Chip*, 2008, **8**, 2188–2196.
99 K. Choi, A. H. C. Ng, R. Fobel, D. A. Chang-Yen, L. E. Yarnell, E. L. Pearson, C. M. Oleksak, A. T. Fischer, R. P. Luoma, J. M. Robinson, J. Audet and A. R. Wheeler, *Anal. Chem.*, 2013, **85**, 9638–9646.
100 A. H. C. Ng, M. Lee, K. Choi, A. T. Fischer, J. M. Robinson and A. R. Wheeler, *Clin. Chem.*, 2015, **61**, 420–429.
101 F. Sassa, K. Morimoto, W. Satoh and H. Suzuki, *Electrophoresis*, 2008, **29**, 1787–1800.
102 A. T. Woolley, K. Lao, A. N. Glazer and R. A. Mathies, *Anal. Chem.*, 1998, **70**, 684–688.
103 J. Wang, B. Tian and E. Sahlin, *Anal. Chem.*, 1999, **71**, 3901–3904.
104 J. Wang, R. Polsky, B. Tian and M. P. Chatrathi, *Anal. Chem.*, 2000, **72**, 5285–5289.
105 M. Pumera, A. Merkoçi and S. Alegret, *TrAC, Trends Anal. Chem.*, 2006, **25**, 219–235.
106 D. C. Kirkpatrick, C. Antwi and R. S. Martin, *Anal. Methods*, 2010, **2**, 811–816.
107 S. K. Kim, H. Lim, T. D. Chung and H. C. Kim, *Sens. Actuators, B*, 2006, **115**, 212–219.
108 C. M. Kang, S. Joo, J. H. Bae, Y.-R. Kim, Y. Kim and T. D. Chung, *Anal. Chem.*, 2011, **84**, 901–907.
109 E. V. Dydek, M. V. Petersen, D. G. Nocera and K. F. Jensen, *J. Electrochem. Soc.*, 2012, **159**, H853–H856.
110 D. Gunasekara, M. Hulvey, S. Lunte and J. Silva, *Anal. Bioanal. Chem.*, 2012, **403**, 2377–2384.
111 R.-G. Wu, C.-S. Yang, C.-C. Cheing and F.-G. Tseng, *Interface Focus*, 2011, **1**, 744–753.
112 Q. L. Zhang, J. J. Xu, H. Z. Lian, X. Y. Li and H. Y. Chen, *Anal. Bioanal. Chem.*, 2006, **384**, 265–270.
113 D. J. Fischer, M. K. Hulvey, A. R. Regel and S. M. Lunte, *Electrophoresis*, 2009, **30**, 3324–3333.
114 D. M. Osbourn and C. E. Lunte, *Anal. Chem.*, 2003, **75**, 2710–2714.
115 R. S. Martin, K. L. Ratzlaff, B. H. Huynh and S. M. Lunte, *Anal. Chem.*, 2002, **74**, 1136–1143.
116 D. B. Gunasekara, M. K. Hulvey and S. M. Lunte, *Electrophoresis*, 2011, **32**, 832–837.
117 C. A. Croushore and J. V. Sweedler, *Lab Chip*, 2013, **13**, 1666–1676.
118 I. A. Ges, R. L. Brindley, K. P. M. Currie and F. J. Baudenbacher, *Lab Chip*, 2013, **13**, 4663–4673.
119 J. L. Erkal, A. Selimovic, B. C. Gross, S. Y. Lockwood, E. L. Walton, S. McNamara, R. S. Martin and D. M. Spence, *Lab Chip*, 2014, **14**, 2023–2032.
120 W. Dungchai, O. Chailapakul and C. S. Henry, *Anal. Chem.*, 2009, **81**, 5821–5826.
121 S. E. Fosdick, M. J. Anderson, C. Renault, P. R. DeGregory, J. A. Loussaert and R. M. Crooks, *Anal. Chem.*, 2014, **86**, 3659–3666.

122 M. D. M. Dryden, D. D. G. Rackus, M. H. Shamsi and A. R. Wheeler, *Anal. Chem.*, 2013, **85**, 8809–8816.
123 J. P. Hart and S. A. Wring, *Electroanalysis*, 1994, **6**, 617–624.
124 C. Hu, X. Bai, Y. Wang, W. Jin, X. Zhang and S. Hu, *Anal. Chem.*, 2012, **84**, 3745–3750.
125 J. J. Shi, F. Tang, H. L. Xing, H. X. Zheng, L. H. Bi and W. Wang, *J. Braz. Chem. Soc.*, 2012, **23**, 1124–1130.
126 S. N. Tan, L. Y. Ge, H. Y. Tan, W. K. Loke, J. R. Gao and W. Wang, *Anal. Chem.*, 2012, **84**, 10071–10076.
127 R. F. Carvalhal, M. Simão Kfouri, M. H. de Oliveira Piazetta, A. L. Gobbi and L. T. Kubota, *Anal. Chem.*, 2010, **82**, 1162–1165.
128 L. Y. Shiroma, M. Santhiago, A. L. Gobbi and L. T. Kubota, *Anal. Chim. Acta*, 2012, **725**, 44–50.
129 A. Apilux, W. Dungchai, W. Siangproh, N. Praphairaksit, C. S. Henry and O. Chailapakul, *Anal. Chem.*, 2010, **82**, 1727–1732.
130 Z. Nie, F. Deiss, X. Liu, O. Akbulut and G. M. Whitesides, *Lab Chip*, 2010, **10**, 3163–3169.
131 C. Renault, M. J. Anderson and R. M. Crooks, *J. Am. Chem. Soc.*, 2014, **136**, 4616–4623.
132 P. Dubois, G. Marchand, Y. Fouillet, J. Berthier, T. Douki, F. Hassine, S. Gmouh and M. Vaultier, *Anal. Chem.*, 2006, **78**, 4909–4917.
133 C. Karuwan, K. Sukthang, A. Wisitsoraat, D. Phokharatkul, V. Patthanasettakul, W. Wechsatol and A. Tuantranont, *Talanta*, 2011, **84**, 1384–1389.
134 S. Lindsay, T. Vazquez, A. Egatz-Gomez, S. Loyprasert, A. A. Garcia and J. Wang, *Analyst*, 2007, **132**, 412–416.
135 Y. H. Yu, J. F. Chen, J. Li, S. Yang, S. K. Fan and J. Zhou, *J. Micromech. Microeng.*, 2013, **23**, 095025.
136 Y. H. Yu, J. F. Chen and J. Zhou, *J. Micromech. Microeng.*, 2014, **24**, 015020.
137 L. C. Clark and C. Lyons, *Ann. N. Y. Acad. Sci.*, 1962, **102**, 29–45.
138 D. Grieshaber, R. MacKenzie, J. Vörös and E. Reimhult, *Sensors*, 2008, **8**, 1400–1458.
139 N. J. Ronkainen, H. B. Halsall and W. R. Heineman, *Chem. Soc. Rev.*, 2010, **39**, 1747–1763.
140 L. D. Mell and J. T. Maloy, *Anal. Chem.*, 1975, **47**, 299–307.
141 B. A. Kuznetsov, G. P. Shumakovich, O. V. Koroleva and A. I. Yaropolov, *Biosens. Bioelectron.*, 2001, **16**, 73–84.
142 *Electrochemical sensors, biosensors and their biomedical applications*, ed. X. Zhang, H. Ju and J. Wang, Academic Press/Elsevier, San Diego, 2008.
143 V. Glezer and O. Lev, *J. Am. Chem. Soc.*, 1993, **115**, 2533–2534.
144 F. Patolsky, Y. Weizmann and I. Willner, *Angew. Chem., Int. Ed.*, 2004, **43**, 2113–2117.
145 M. Zayats, E. Katz, R. Baron and I. Willner, *J. Am. Chem. Soc.*, 2005, **127**, 12400–12406.
146 D. Purvis, O. Leonardova, D. Farmakovsky and V. Cherkasov, *Biosens. Bioelectron.*, 2003, **18**, 1385–1390.
147 K. Liang, W. Mu, M. Huang, Z. Yu and Q. Lai, *Electroanalysis*, 2006, **18**, 1505–1510.
148 L. Yang, Y. Li and G. F. Erf, *Anal. Chem.*, 2004, **76**, 1107–1113.
149 G. Pampalakis and S. O. Kelley, *Analyst*, 2009, **134**, 447–449.
150 X. Li, Z. Nie, C. Cheng, A. Goodale and G. Whitesides, Proc. Micro Tot. Anal. Sys., 2010, *Chemical and Biological Microsystems Society*, 2010, vol. 3, pp. 1487–1489.
151 Y. Astier and P. N. Bartlett, *Bioelectrochemistry*, 2004, **64**, 15–22.
152 C. G. Bauer, A. V. Eremenko, E. Ehrentreich-Förster, F. F. Bier, A. Makower, H. B. Halsall, W. R. Heineman and F. W. Scheller, *Anal. Chem.*, 1996, **68**, 2453–2458.
153 A. Bange, H. B. Halsall and W. R. Heineman, *Biosens. Bioelectron.*, 2005, **20**, 2488–2503.
154 A. Bhimji, A. A. Zaragoza, L. S. Live and S. O. Kelley, *Anal. Chem.*, 2013, **85**, 6813–6819.
155 A. De La Escosura-Muñiz and A. Merkoçi, *Small*, 2011, **7**, 675–682.
156 A. De La Escosura-Muñiz and A. Merkoçi, *Electrochem. Commun.*, 2010, **12**, 859–863.
157 B. T. T. Nguyen, A. E. K. Peh, C. Y. L. Chee, K. Fink, V. T. K. Chow, M. M. L. Ng and C.-S. Toh, *Bioelectrochemistry*, 2012, **88**, 15–21.
158 R. M. Umek, S. W. Lin, J. Vielmetter, R. H. Terbrueggen, B. Irvine, C. J. Yu, J. F. Kayyem, H. Yowanto, G. F. Blackburn, D. H. Farkas and Y.-P. Chen, *J. Mol. Diagn.*, 2001, **3**, 74–84.
159 C. Fan, K. W. Plaxco and A. J. Heeger, *Proc. Natl. Acad. Sci. U. S. A.*, 2003, **100**, 9134–9137.
160 E. Paleček, *Nature*, 1960, **188**, 656–657.
161 M. H. Shamsi and H.-B. Kraatz, *Analyst*, 2011, **136**, 3107–3112.
162 M. H. Shamsi and H.-B. Kraatz, *Analyst*, 2010, **135**, 2280–2285.
163 M. H. Shamsi and H.-B. Kraatz, *Analyst*, 2011, **136**, 4724–4731.
164 M. N. Alam, M. H. Shamsi and H.-B. Kraatz, *Analyst*, 2012, **137**, 4220–4225.
165 X. R. Cheng, B. Y. H. Hau, T. Endo and K. Kerman, *Biosens. Bioelectron.*, 2014, **53**, 513–518.
166 S. O. Kelley, E. M. Boon, J. K. Barton, N. M. Jackson and M. G. Hill, *Nucleic Acids Res.*, 1999, **27**, 4830–4837.
167 A. Erdem, K. Kerman, B. Meric, U. S. Akarca and M. Ozsoz, *Electroanalysis*, 1999, **11**, 586–587.
168 A. B. Steel, T. M. Herne and M. J. Tarlov, *Anal. Chem.*, 1998, **70**, 4670–4677.
169 M. A. Lapierre, M. O'Keefe, B. J. Taft and S. O. Kelley, *Anal. Chem.*, 2003, **75**, 6327–6333.
170 L. Soleymani, Z. Fang, X. Sun, H. Yang, B. J. Taft, E. H. Sargent and S. O. Kelley, *Angew. Chem., Int. Ed.*, 2009, **48**, 8457–8460.
171 K. B. Cederquist and S. O. Kelley, *Curr. Opin. Chem. Biol.*, 2012, **16**, 415–421.
172 J. Das and S. O. Kelley, *Anal. Chem.*, 2013, **85**, 7333–7338.
173 J. D. Besant, J. Das, E. H. Sargent and S. O. Kelley, *ACS Nano*, 2013, **7**, 8183–8189.
174 I. Ivanov, J. Stojcic, A. Stanimirovic, E. Sargent, R. K. Nam and S. O. Kelley, *Anal. Chem.*, 2012, **85**, 398–403.
175 B. Lam, Z. Fang, E. H. Sargent and S. O. Kelley, *Anal. Chem.*, 2011, **84**, 21–25.

176 Y. Xiao, A. A. Lubin, B. R. Baker, K. W. Plaxco and A. J. Heeger, *Proc. Natl. Acad. Sci. U. S. A.*, 2006, **103**, 16677–16680.
177 Y. Xiao, B. D. Piorek, K. W. Plaxco and A. J. Heeger, *J. Am. Chem. Soc.*, 2005, **127**, 17990–17991.
178 Y. Xiao, A. A. Lubin, A. J. Heeger and K. W. Plaxco, *Angew. Chem., Int. Ed.*, 2005, **44**, 5456–5459.
179 J. Das, K. B. Cederquist, A. A. Zaragoza, P. E. Lee, E. H. Sargent and S. O. Kelley, *Nat. Chem.*, 2012, **4**, 642–648.
180 J. Heo and R. M. Crooks, *Anal. Chem.*, 2005, **77**, 6843–6851.
181 A. Kratz, M. Ferraro, P. M. Sluss and K. B. Lewandrowski, *N. Engl. J. Med.*, 2004, **351**, 1548–1563.
182 K. Mitsakakis and E. Gizeli, *Anal. Chim. Acta*, 2011, **699**, 1–5.
183 S. Rothkrantz-Kos, M. P. J. Schmitz, O. Bekers, P. P. C. A. Menheere and M. P. van Dieijen-Visser, *Clin. Chem.*, 2002, **48**, 359–362.
184 F. Kato, H. Ogi, T. Yanagida, S. Nishikawa, M. Hirao and M. Nishiyama, *Biosens. Bioelectron.*, 2012, **33**, 139–145.
185 H. I. Peng, C. M. Strohsahl and B. L. Miller, *Lab Chip*, 2012, **12**, 1089–1093.
186 L. M. Lechuga, J. Tamayo, M. Álvarez, L. G. Carrascosa, A. Yufera, R. Doldán, E. Peralías, A. Rueda, J. A. Plaza, K. Zinoviev, C. Domínguez, A. Zaballos, M. Moreno, C. Martínez-A, D. Wenn, N. Harris, C. Bringer, V. Bardinal, T. Camps, C. Vergnenègre, C. Fontaine, V. Díaz and A. Bernad, *Sens. Actuators, B*, 2006, **118**, 2–10.
187 H. Arata, H. Komatsu, K. Hosokawa and M. Maeda, *PLoS One*, 2012, **7**, e48329.
188 A. Persat and J. G. Santiago, *Anal. Chem.*, 2011, **83**, 2310–2316.
189 A. Apilux, Y. Ukita, M. Chikae, O. Chailapakul and Y. Takamura, *Lab Chip*, 2013, **13**, 126–135.
190 V. Nicolas, W. Daan, C. Frederik, V. Steven, V. Bert, P. Robert and L. Jeroen, *J. Micromech. Microeng.*, 2011, **21**, 054026.
191 L. Malic, T. Veres and M. Tabrizian, *Biosens. Bioelectron.*, 2009, **24**, 2218–2224.
192 I. J. Chen and I. M. White, *Biosens. Bioelectron.*, 2011, **26**, 4375–4381.
193 F. Lamberti, C. Luni, A. Zambon, P. A. Serra, M. Giomo and N. Elvassore, *Biomicrofluidics*, 2012, **6**, 024114.
194 A. Wisitsoraat, P. Sritongkham, C. Karuwan, D. Phokharatkul, T. Maturos and A. Tuantranont, *Biosens. Bioelectron.*, 2010, **26**, 1514–1520.
195 N. Ruecha, W. Siangproh and O. Chailapakul, *Talanta*, 2011, **84**, 1323–1328.
196 B. V. Chikkaveeraiah, H. Y. Liu, V. Mani, F. Papadimitrakopoulos and J. F. Rusling, *Electrochem. Commun.*, 2009, **11**, 819–822.
197 J. Yan, V. A. Pedrosa, J. Enomoto, A. L. Simonian and A. Revzin, *Biomicrofluidics*, 2011, **5**, 03208.
198 Z. Matharu, J. Enomoto and A. Revzin, *Anal. Chem.*, 2013, **85**, 932–939.
199 D. Itoh, F. Sassa, T. Nishi, Y. Kani, M. Murata and H. Suzuki, *Sens. Actuators, B*, 2012, **171**, 619–626.
200 G. A. Messina, N. V. Panini, N. A. Martinez and J. Raba, *Anal. Biochem.*, 2008, **380**, 262–267.
201 S. Viswanathan, C. Rani, A. V. Anand and J. A. A. Ho, *Biosens. Bioelectron.*, 2009, **24**, 1984–1989.
202 C. Kellner, M. L. Botero, D. Latta, K. Drese, A. Fragoso and C. K. O'Sullivan, *Electrophoresis*, 2011, **32**, 926–930.
203 D. Berdat, A. C. M. Rodriguez, F. Herrera and M. A. M. Gijs, *Lab Chip*, 2008, **8**, 302–308.
204 P. Lin, X. Luo, I. M. Hsing and F. Yan, *Adv. Mater.*, 2011, **23**, 4035–4040.
205 J. S. Swensen, Y. Xiao, B. S. Ferguson, A. A. Lubin, R. Y. Lai, A. J. Heeger, K. W. Plaxco and H. T. Soh, *J. Am. Chem. Soc.*, 2009, **131**, 4262–4266.
206 Y. Liu, T. Kwa and A. Revzin, *Biomaterials*, 2012, **33**, 7347–7355.
207 T. Kwa, Q. Zhou, Y. Gao, A. Rahimian, L. Kwon, Y. Liu and A. Revzin, *Lab Chip*, 2014, **14**, 1695–1704.
208 Z. Matharu, D. Patel, Y. Gao, A. Haque, Q. Zhou and A. Revzin, *Anal. Chem.*, 2014, 8865–8872.
209 T.-H. Kim, K. Abi-Samra, V. Sunkara, D.-K. Park, M. Amasia, N. Kim, J. Kim, H. Kim, M. Madou and Y.-K. Cho, *Lab Chip*, 2013, **13**, 3747–3754.
210 C. Zhao, M. M. Thuo and X. Y. Liu, *Sci. Technol. Adv. Mater.*, 2013, **14**, 054402.
211 M. D. Hughes, *J. Diabetes Sci. Technol.*, 2009, **3**, 1219–1223.
212 Cartridge and Test Information Sheets, www.abbottpointofcare.com/Customer-Info-Center/Cartridge-and-Test-Info-Sheets.aspx, accessed August 19, 2014.
213 Nanomix, www.nano.com, accessed 21 August 2014.
214 Daktari Diagnostics, http://daktaridx.com, accessed 19 August 2014.
215 GeneFluidics, www.genefluidics.com, accessed 21 August 2014.

